Pergamon

Geochimica et Cosmochimica Acta, Vol. 66, No. 9, pp. 1663–1679, 2002

0016-7037/02 $22.00 + .00

PII S0016-7037(01)00871-7

# Chemistry of glass inclusions in olivines of the CR chondrites Renazzo, Acfer 182, and El Djouf 001

MARIA EUGENIA VARELA,[1,*] GERO KURAT,[2] PETTER HOPPE,[3] and FRANZ BRANDSTÄTTER[2]

[1]CONICET- UNS, Departamento de Geologia, San Juan 670 (8000) Bahia Blanca, Argentina
[2]Naturhistorisches Museum, Postfach 417, A-1014, Vienna, Austria
[3]Abteilung Kosmochemie, Max-Planck-Institute für Chemie, Postfach 3060, D-55020 Mainz, Germany

(*Received March* 27, 2001; *accepted in revised form November* 2, 2001)

**Abstract**—Glass inclusions in olivines of the Renazzo, El Djouf 001, and Acfer 182 CR-type chondrites are chemically divers and can be classified into Al-rich, Al-poor, and Na-rich types. The chemical properties of the glasses are independent of the occurrence of the olivine (isolated or part of an aggregate or chondrule) and its composition. The glasses are silica-saturated (Al-rich) or oversaturated (Al-poor, 24% normative quartz). All glasses have chondritic $CaO/Al_2O_3$ ratios, unfractionated CI-normalized abundances of refractory trace elements and are depleted in moderately volatile and volatile elements. Thus the glasses are likely to be of a primitive condensate origin whose chemical composition has been established before chondrule formation and accretion, rather then the product of either crystal fractionation from chondrule melts or part melting of chondrules. Rare Na-rich glasses give evidence for elemental exchange between the glass and a vapor phase. Because they have $Al_2O_3$ contents and trace element abundances very similar to those of the Al-rich glasses, they likely were derived from the latter by Ca exchange (for Na) with the nebula. Elemental exchange reactions also have affected practically all olivines (e.g., exchange of Mg of olivine for $Fe^{2+}$, $Mn^{2+}$, and $Cr^{3+}$). Glasses formed contemporaneously with the host olivine. As the most likely process for growing nonskeletal olivines from a vapor we consider the VLS (vapor–liquid–solid) growth process, or liquid-phase epitaxy. Glasses are the possible remnants of the liquid interface between growing crystal and the vapor. Such liquids can form stably or metastably in regions with enhanced oxygen fugacity as compared to that of a nebula of solar composition. *Copyright © 2002 Elsevier Science Ltd*

## 1. INTRODUCTION

The genesis of Ca-Al-rich glass inclusions in olivines of carbonaceous chondrites is a matter of ongoing debate. Those found in the Murchison chondrite led Fuchs et al. (1973) to suggest that such glass inclusions could be the result of a condensation process that formed the olivine. In contrast, McSween (1977) and Roedder (1981) considered them to be trapped remnants of a parent liquid, in this case they could be the product of fractional crystallization of chondrule melts. However, the first trace element analysis done on glass inclusions in a carbonaceous chondrites (two glass inclusions in olivine from the Renazzo chondrite) by Kurat et al. (1997) strongly supported a condensation origin of the glass inclusions. Thus, if this hypothesis is correct, variations in the chemical composition of the glasses could reflect processes in the early solar nebula.

The importance of the Renazzo chondrite was already pointed out by Wood (1962) who first noticed the coexistence, in this stone, of highly unequilibrated phases. Besides the Renazzo samples, we have studied glass inclusions in olivines of some other related chondrites such as: El Djouf 001 (henceforth shortened to El Djouf) with similar elemental and isotopic compositions to that of CR chondrites (Bischoff et al., 1993) and classified as a CR chondrite by Kallemeyn et al. (1994) and Weisberg et al. (1993), and the ungrouped meteorite Acfer 182 which shares petrographic and isotopic features with CR chondrites (Bischoff et al., 1993; Kallemeyn et al., 1994; Acfer 182 has recently been reclassified as CH chondrite—Bischoff, 2001).

Here we present the results of a major and trace element study of glass inclusions in olivines of these chondrites which belong to the CR (Renazzo-type) group, which is characterized by having "pervasive presence of phases (phyllosilicates, magnetite) produced by hydrothermal alteration, high and variable Ni contents in chondrule-interior metal, and zoning in matrix and chondrule surface metal indicating minor reduction during the mild metamorphism that preceded the aqueous alteration" (Kallemeyn et al., 1994). However, glass inclusions appear to behave as relatively closed systems which mostly escaped the metasomatic processes that affected most chondrite constituents.

This paper focuses on the implications of the chemical variations in glasses of glass inclusions and discusses the possible genesis of the glass inclusions in olivines.

## 2. ANALYTICAL TECHNIQUES

This study of glass inclusions in olivines comprises a study of the petrography of the inclusions (e.g., occurrence, phase abundances, chemistry of the glass, etc.), of the host olivines, and of the aggregates and chondrules containing these olivines. Generally, the glass inclusions are located at different depths in the olivine. To obtain the maximum information possible from a sample, we proceeded as follows: the selected inclusions were brought to the surface by polishing the section to the right level and then analyzed by different techniques as described below.

* Author to whom correspondence should be addressed (evarela@criba.edu.ar).

The sample was then repolished, using a procedure that removes only a few micrometers at a time until new glass inclusions appeared at the surface.

Analytical scanning electron microscopy was performed with a JEOL-6400 instrument (NHM, Vienna) with a sample current of 1 nA and an accelerating voltage of 15 kV. Major element compositions of glasses were measured with CAMECA Camebax (Center d'analyses Camparis, Université de Paris VI) and SX50 (Atomic Energy Commission, Buenos Aires, Argentina) electron microprobes. Analyses were performed using a defocused beam (5 $\mu$m), an acceleration voltage of 15 kV, and a sample current of 10 nA. The samples were first analyzed for Na with a counting time of 5 s, followed by all other elements with counting times of 10 s. The precision was established by analyzing basaltic and trachytic glasses (ALV 981 R24 and CFA 47; Métrich and Clocchiatti, 1989) and corrections were made using the online ZAF program.

Trace element abundances in glasses and host olivines were measured with the modified Cameca IMS3f ion microprobes in Bern (Physikalisches Institut, Universität Bern) and in Mainz (Abteilung Kosmochemie, Max-Planck-Institut für Chemie). The samples were sputtered with a 17-keV primary $O^-$ ion beam of 1 to 5 nA and $\approx$10 $\mu$m diameter (glass inclusions) and 10 nA and $\approx$15 to 20 $\mu$m diameter (host olivines). Energy filtering was applied (100 eV energy offset relative to low-energy edge of $^{16}O^+$ secondary ions) to suppress contributions from molecular interferences to the secondary ion signals. Secondary ions of K, Sc (in some cases), Ti, V, Cr, Sr, Y, Zr, Nb, Ba, the rare earth elements (REE), and Hf were measured in the peak-jumping mode, and elemental concentrations were calculated following the procedure of Zinner and Crozaz (1986).

## 3. SAMPLES

We have studied the following samples: polished thin sections (PTS) Renazzo L3812, Renazzo L3824, Renazzo 11, 12, 13, Renazzo v. A238 and Acfer 182 (all from the NHM, Vienna) and El Djouf 001 (AMNH, New York). The glass inclusions usually consist of glass plus a bubble, have sizes from 10 to 80 $\mu$m, with a main population between 20 to 30 $\mu$m, and occur in isolated olivines and olivines of aggregates or chondrules.

## 4. RESULTS

### 4.1. Definitions

Before giving any description of the petrography of inclusions and the host olivines, we need to introduce the reader to the definitions used to classify inclusions in minerals and how to distinguish chondrules from aggregates. Minerals can contain several generations of inclusions, which are usually classified as "primary" and "secondary" inclusions (Roedder, 1984). Primary inclusions are typically single inclusions or form small groups of inclusions (cluster) in an otherwise inclusion-free crystal. Consequently, primary inclusions are imperfections in an otherwise perfect crystal (Roedder, 1984). As these inclusions represent "accidents" in the normal process of crystal growth, their distribution in a crystal may be essentially random. Primary inclusions are contemporaneously formed with their host.

Secondary inclusions typically occur in trails and usually contain trapped fluids which provided healing of the previously fractured crystal. Consequently, they can be introduced at any time after the formation of the crystal and carry no information on the crystal growth conditions. Under specific growth conditions of crystals, however, trails of primary inclusions can form which consequently are called "pseudosecondary" inclusions.

Olivine is the principal phase carrying inclusions in chondritic meteorites and is a major phase of chondrite constituents. In this report we distinguish:

- isolated olivines—single crystals in the chondrite matrix;
- olivines in chondrules, round, droplet-shaped objects that have apparently been at least partly molten in the course of their history ("droplet chondrule" in American terminology, Gooding and Keil, 1981);
- olivines in aggregates, irregularly shaped angular to rounded aggregations of minerals with porous to dense (recrystallized) matrix.

### 4.2. Petrography and Chemical Composition of Glass Inclusions and Host Olivines

#### *4.2.1. Renazzo (PTS Renazzo L3812, Renazzo L3824, Renazzo A238, Renazzo 11, 12, and 13)*

Glass inclusions are isolated or form clusters in olivines of aggregates, chondrules, or in isolated olivine (Fig. 1). Glass inclusions consist of either clear glass plus shrinkage bubble, or clear glass plus shrinkage bubble plus a metal globule (Fe: 86 - Ni:12.6 wt.%; inclusion R27), or clear glass plus a spinel crystal, or brownish devitrified glass plus shrinkage bubble.

Clear glass inclusions can be divided into two groups on the basis of their contents of $Al_2O_3$ and $SiO_2$ (Table 1). One group, from here on called the Al-rich group, has $SiO_2$ contents varying from ~39 to 52 wt.% (average 44.2 wt.%) and $Al_2O_3$ contents from ~22.7 to 28.8 wt.% (average 27 wt.%). Other major elements content varies somewhat in this group: CaO from 15 to 26 wt.% (average 21.7 wt.%), $TiO_2$ from 0.8 to 1.8 wt.% (average 1.3 wt.%), and MgO from 3.3 to 4.9 wt.% (average 4 wt.%).

The second group, called "Al-poor," has $SiO_2$ contents higher than 55 wt.% (average 59 wt.%) and $Al_2O_3$ contents lower than 21 wt.% (average 18.9 wt.%). The CaO content varies from 6.7 to 19 wt.% (average 15.6 wt.%), that of $TiO_2$ and MgO between 0.2 and 1.4 wt.% (average 0.8 wt.%) and 2 and 7.2 wt.% (average 3.2 wt.%), respectively. In the Al-rich and the Al-poor groups of glasses, the alkali content is low. It is very low in the Al-rich glasses ($Na_2O < 0.5$ wt.%, commonly below the detection limit of the electron microprobe, ~0.02 wt.%) and slightly higher in the Al-poor glasses (<0.02 to 2.6 wt.%, average 0.5 wt.% $Na_2O$). These glasses have approximately chondritic $CaO/Al_2O_3$ ratios (Varela and Kurat, 2000) (Fig. 2a).

A third chemical group of glasses could be considered as an Na-rich, Ca-poor subgroup of the Al-rich glasses and we will refer to them as Na-rich glasses. They have varying $SiO_2$ contents between 46 and 55 wt.% and $Al_2O_3$ contents between

(a)

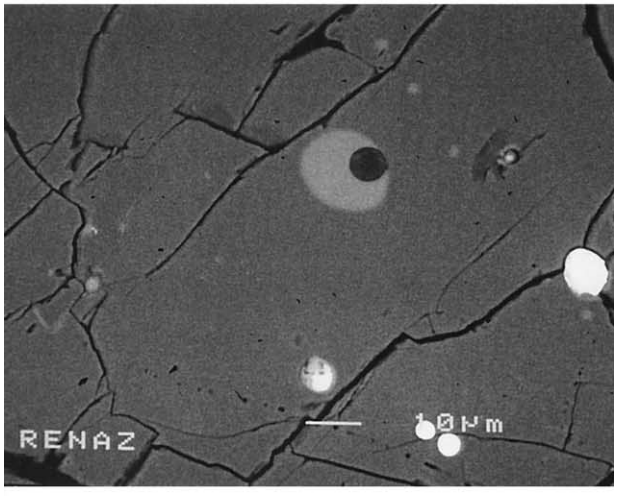


(b)

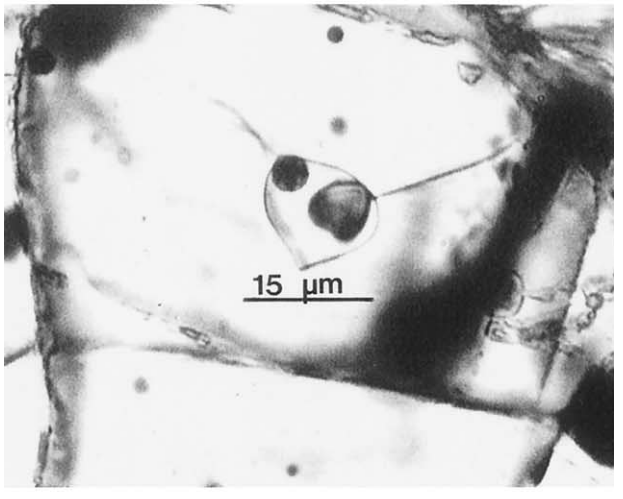


(c)

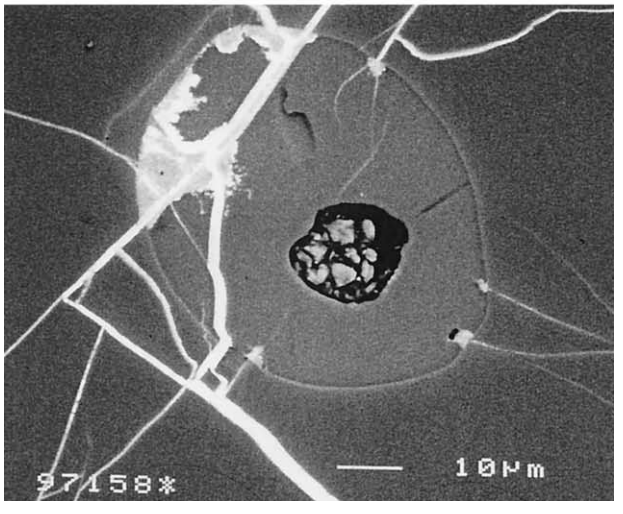


23.8 and 29.6 wt.%. They have similar contents of FeO and MgO as compared to the Al-rich and Al-poor glass inclusions but are poor in CaO (0.9 to 8.5 wt.%), have highly variable contents of $TiO_2$ (0.2 to 2 wt.%), and have high contents of $Na_2O$ (4.5 to 14.7 wt.%). A profile of 15 points made by ASEM in one of these glass inclusions (R15, size ~55 $\mu$m) shows no variation in the alkali contents of the glass over the profile.

All Na-rich inclusions are devitrified brownish inclusions, except one (R15). Glass inclusion R15 has a clear glass and is crossed by several fractures (Fig. 1c). All Na-rich inclusions were found in the PTS Renazzo 12. In this sample, devitrified glass inclusions and inclusions containing small spinel crystals are overabundant as compared to all other samples.

Most glass inclusions are hosted by olivines with FeO and $Cr_2O_3$ contents varying from 0.1 to 3.6 wt.% and 0.1 to 0.78 wt.%, respectively (Table 1). Olivines are parts of aggregates or chondrules with the following textures: porphyritic olivine-pyroxene (POP: R2, R3, R4, R6, R7, R8, R9, R10, R16, R17, R19, R22, R23, R24, R25), porphyritic pyroxene-olivine (PPO, with poikilitic pyroxenes: R20, R26), and mosaic olivine (MO: R11, R12, R13, R14, R15, R18, R21, R27). The mosaic texture is formed by few euhedral to subhedral olivines, 300 to 500 $\mu$m in diameter, forming an aggregate (R27) or chondrule (as in the case of inclusion R15). In some cases aggregates have large olivines in the center surrounded by a shell of small olivine grains (50 to 150 $\mu$m) with very few or without pyroxenes (R11, R14, R27). Only one host olivine is an isolated olivine (R5, Table 1).

### *4.2.2. El Djouf 001*

Two glass inclusions have been analyzed in this sample, ED1 and ED2 (Table 1). Both inclusions are 25 to 30 $\mu$m in size and are composed of clear glass and a shrinkage bubble. In both cases, these glass inclusions are not only single inclusions in the crystal but also the only inclusion observed in the aggregate or chondrule. Based on their $SiO_2$ and $Al_2O_3$ contents, which vary from 60 to 65 wt.% and 18.5 to 17.5 wt.%, respectively, both glass inclusions belong to the Al-poor group (Table 1) as defined for Renazzo inclusions. Host olivines of glass inclusions ED1 and ED2 are part of an aggregate and of a chondrule, respectively, both with porphyritic textures. They have FeO contents of 3.6 and 1.9 wt.% and $Cr_2O_3$ contents of 0.78 and 0.45 wt.%, respectively.

### *4.2.3. Acfer 182*

Five primary glass inclusions with sizes varying from 10 to 40 $\mu$m were analyzed in the Acfer 182 sample. Inclusion Acfer1 consists of clear glass plus a spinel crystal. Acfer2 is a devitrified glass inclusion, and Acfer3 to Acfer5 are clear glass inclusions. All inclusions have a shrinkage bubble.

Fig. 1. (a) Glass inclusion with bubble in Renazzo olivine (glass R10, sample Renazzo L3428). Bright blebs are Fe, Ni metal inclusions. BSE image. (b) Glass inclusion with bubble (spherical) in Renazzo olivine (glass R27, sample Renazzo 13). Large heart-shaped dark area is ion microprobe ablation pit. Transmitted light picture. (c) Glass inclusion with bubble in Renazzo olivine (glass R15, sample Renazzo 12). Note fractures that reach the glass inclusion. BSE image.

Table 1. Representative major element composition of glasses of glass inclusions in olivines of the Renazzo, EI Djouf 001, and Acfer 182, CR-type carbonaceous chondrites (Electron Microprobe Analysis in wt.%).

| | Al-rich | | | | | | | | | | | | | | Na-rich | | | |
|---|---|---|---|---|---|---|---|---|---|---|---|---|---|---|---|---|---|---|
| | R1 | R2[a] | R3[a] | R4 | R5[a] | R6[a] | R7[a] | R8 | R9 | R10 | R11 | Acfer1 | Acfer3 | Acfer4 | R12 | R13 | R14 | R15[a] |
| $SiO_2$ | 51.0 | 42.1 | 41.6 | 39.2 | 44.7 | 40.4 | 45.6 | 45.0 | 47.9 | 44.0 | 49.9 | 46.6 | 51.6 | 43.7 | 46.2 | 50.8 | 55.1 | 54.9 |
| $TiO_2$ | 0.8 | 1.3 | 1.3 | 1.3 | 1.8 | 1.3 | 1.2 | 1.5 | 1.5 | 1.2 | 1.0 | 1.2 | 1.3 | 1.3 | 2.0 | 1.3 | 0.9 | 0.2 |
| $Al_2O_3$ | 27.2 | 27.6 | 27.7 | 28.8 | 26.1 | 28.3 | 26.1 | 27.0 | 25.2 | 26.4 | 22.7 | 23.9 | 22.8 | 28.1 | 27.0 | 29.6 | 27.7 | 23.8 |
| $Cr_2O_3$ | nd | 0.3 | 0.3 | 0.1 | 0.4 | 0.0 | 0.1 | nd | nd | 0.2 | 0.5 | nd | 0.7 | 0.1 | 0.1 | 0.2 | 0.6 | 0.3 |
| FeO | 0.5 | 0.7 | 0.6 | 0.1 | 0.9 | 0.1 | 0.2 | 0.9 | 0.7 | 0.1 | 1.7 | 0.8 | 1.5 | 0.7 | 3.9 | 1.6 | 0.6 | 2.2 |
| MnO | 0.1 | 0.1 | nf | 0.1 | nd | nd | nd | 0.0 | 0.2 | 0.0 | 0.2 | nf | nf | 0.0 | nd | 0.0 | nd | 0.1 |
| MgO | 3.5 | 4.8 | 4.9 | 4.0 | 3.5 | 3.9 | 3.9 | 4.6 | 3.4 | 3.3 | 4.0 | 4.1 | 4.2 | 3.9 | 1.9 | 0.7 | 2.8 | 1.1 |
| CaO | 15.1 | 22.4 | 21.6 | 26.3 | 20.7 | 28.3 | 22.5 | 21.0 | 19.4 | 24.2 | 17.8 | 21.8 | 17.8 | 22.2 | 1.4 | 1.0 | 8.5 | 3.3 |
| $Na_2O$ | 0.0 | nf | nf | 0.1 | nd | 0.0 | nd | nd | nd | nd | 0.4 | nf | nf | nf | 14.7 | 14.2 | 4.5 | 11.1 |
| $K_2O$ | nd | nf | nf | nd | 0.0 | nd | nd | 0.1 | 0.0 | nd | 0.0 | nd | nf | nf | 2.1 | 0.5 | 0.1 | 1.3 |
| $P_2O_5$ | 0.3 | 0.3 | 0.3 | 0.3 | nd | 0.2 | 0.2 | 0.5 | 0.3 | nd | nd | 0.0 | 0.1 | nf | nd | 0.0 | 0.1 | 0.2 |
| Total | 98.5 | 99.6 | 98.3 | 100.2 | 98.2 | 97.5 | 99.7 | 100.5 | 98.5 | 99.4 | 98.2 | 98.5 | 99.9 | 99.9 | 99.2 | 100.0 | 100.8 | 98.5 |
| FeO Host | 1.2 | 0.9 | 0.9 | 0.1 | 2.2 | 0.2 | 0.2 | 1.7 | 0.7 | 0.5 | 2.4 | 1.2 | 2.5 | 0.9 | 0.4 | 0.7 | 1.3 | |
| $Cr_2O_3$ Host | nd | 0.3 | 0.3 | 0.1 | 0.3 | nd | nd | nd | nd | 0.2 | 0.7 | 0.2 | 0.5 | 0.3 | 0.1 | 0.3 | 0.2 | 0.6 |
| Texture | Aggr MO | Aggr POP | Aggr POP | Aggr POP | IO | Aggr POP | Aggr POP | Aggr POP | Aggr POP | Aggr POP | Aggr MO | Aggr MO | IO | IO | Aggr MO | Aggr MO | Aggr MO | Ch MO |
| An (CT-°C) | 1424 | 1561 | 1564 | 1647 | 1502 | 1602 | 1501 | 1512 | 1453 | 1533 | 1384 | 1455 | 1379 | 1547 | — | — | 1317 | — |
| An + Aug (CT-°C) | 1188 | 1350 | 1346 | 1574 | 1263 | 1457 | 1290 | 1281 | 1222 | 1328 | 1211 | 1266 | 1204 | 1316 | — | — | 1167 | — |

Acfer2, 3, and 4 glass inclusions are hosted by isolated olivines (200 to 350 $\mu$m in size). The host olivine of Acfer1 is part of an aggregate of anhedral olivines of 50 to150 $\mu$m size with very few pyroxenes. The host olivine of Acfer5 is part of an aggregate with euhedral to subhedral olivines (30 to ~100 $\mu$m) in a mosaic texture. There is little matrix in this aggregate and it is free of alteration. Host olivines of all five inclusions have FeO and $Cr_2O_3$ contents varying from 0.65 to 1.47 wt.% and 0.12 to 0.65 wt.%, respectively (Table 1).

Acfer1, 3, and 4 have $SiO_2$ and $Al_2O_3$ contents of 43.2 to 51.6 wt.% and 22.8 to 28.1 wt.%, respectively, and belong to the Al-rich group as defined for Renazzo inclusions. Acfer2 and Acfer5 have high contents of $SiO_2$ (57.5 and 66.2 wt.%) and low content of $Al_2O_3$ (19.8 and 13.6 wt.%) and belong to the Al-poor group.

### 4.3. Trace Element Contents of Glass Inclusions and Host Olivines

Trace element contents could be measured only in the largest and best-exposed glasses of the following glass inclusions: R2, R3, R5, R6, and R7 (Al-rich group); R17, R27 (Al-poor group), and R15 (Na-rich group). The trace element contents of the host olivines were also measured. Results are given in Table 2.

The refractory trace element contents of the Al-rich glasses are high, between 10 and 20 $\times$ CI abundances and have mostly unfractionated patterns (Fig. 3a). Only glass R7 displays some abundance anomalies: Tm seems to be overabundant and Yb depleted with respect to the other REE. Vanadium and Cr are depleted in all glasses relative to the refractory trace elements with abundances varying from 0.2 to 1 $\times$ CI abundances.

The Al-poor glasses are also trace element–rich (Fig. 3b) with a variety of abundance patterns. Glass R27 has a flat trace element pattern with a hint of a positive Eu anomaly. Glass R17 has a fractionated trace element abundance pattern with REE abundances increasing from light REE (LREE) to heavy REE (HREE) and with a strong negative Eu anomaly. In addition, the abundances of Zr and Ti are fractionated relative to each other and to the LREE. Both glasses are strongly depleted in V and Cr relative to the refractory element abundances. The Sr content is depleted in glass R17 relative to the refractory trace elements but is not depleted in glass R27.

Trace element contents of the Na-rich glass R15 are also high, 10 to 20 $\times$ CI abundances, with the exception of Ti, Eu, Ba, Sr, V, and Cr which are depleted with respect to the refractory lithophile elements (Fig. 3b, Table 2).

Trace element abundances in olivines (Fig. 3) are variable but usually low and fractionated with respect to chondritic abundances. Abundances of most trace elements vary widely with Ti, V, Cr, and the HREE ranging from 0.1 to 1 $\times$ CI, all other elements measured having abundances $<0.1 \times$ CI abundances.

## 5. DISCUSSION

### 5.1. Glass Inclusions and Interstitial Glasses

Glasses of glass inclusions in minerals and those present as interstitial glasses have usually comparable compositions (e.g., in upper mantle xenoliths as well as in chondrules). Because of this, it is generally assumed that glass inclusions and interstitial glasses provide similar information about fine scale melting and crystallization. However, the two systems are in fact quite different and can provide quite different information (Schiano and Bourdon, 1999). Glass inclusions are simple systems, they are formed during growth of the host, and they are in contact with a single mineral phase. Conversely, interstitial glasses are irregular domains along grain boundaries, are in contact with several phases and behave as open systems and therefore record the latest changes during the formation of the rock. On the other hand, glass inclusions are isolated closed systems and they record conditions prevailing during formation of the host.

Even if the glass inclusions and the interstitial glasses formed from the same melt, their memory will be related to

Table 1. (Continued)

| | Al-poor group | | | | | | | | | | | | | | | |
|---|---|---|---|---|---|---|---|---|---|---|---|---|---|---|---|---|
| | R16 | R17[a] | R18 | R19 | R20 | R21 | R22 | R23 | R24 | R25 | R26 | R27[a] | Acfer2 | Acfer5 | ED1 | ED2 |
| $SiO_2$ | 55.0 | 58.5 | 56.7 | 60.5 | 60.3 | 61.5 | 58.2 | 57.1 | 57.7 | 59.3 | 62.5 | 57.5 | 66.2 | 57.5 | 60.0 | 65.2 |
| $TiO_2$ | 1.1 | 1.4 | 0.6 | 0.9 | 0.7 | 0.6 | 1.1 | 0.8 | 1.1 | 0.7 | 0.5 | 0.8 | 0.6 | 1.1 | 0.9 | 0.2 |
| $Al_2O_3$ | 20.5 | 18.6 | 19.4 | 17.9 | 17.3 | 15.5 | 19.3 | 21.1 | 19.0 | 17.5 | 17.2 | 20.4 | 13.6 | 19.8 | 18.5 | 17.5 |
| $Cr_2O_3$ | 0.4 | 0.5 | 0.2 | nd | 0.5 | nd | 0.5 | 0.4 | 0.4 | 0.5 | 0.6 | 0.3 | nd | 0.3 | 0.7 | 0.5 |
| FeO | 0.5 | 0.5 | 0.3 | 2.5 | 0.7 | 1.5 | 1.3 | 0.6 | 0.7 | 4.1 | 0.6 | 1.1 | 1.0 | 1.1 | 1.3 | 0.5 |
| MnO | nd | 0.0 | 0.0 | 0.0 | 0.2 | 0.2 | 0.1 | nd | 0.2 | 0.3 | 0.0 | 0.1 | 0.0 | 0.1 | 0.1 | nf |
| MgO | 2.0 | 3.1 | 3.2 | 3.5 | 3.7 | 5.1 | 3.1 | 2.7 | 3.2 | 3.6 | 3.9 | 3.0 | 4.6 | 4.3 | 3.0 | 3.0 |
| CaO | 16.3 | 17.0 | 19.2 | 14.6 | 15.3 | 14.7 | 15.7 | 16.4 | 18.3 | 13.4 | 13.2 | 15.2 | 12.3 | 16.0 | 14.9 | 13.1 |
| $Na_2O$ | 2.6 | 0.2 | 0.0 | nf | 0.0 | 0.1 | 0.4 | 0.6 | nd | 0.3 | nd | 0.3 | 0.1 | 0.1 | 0.2 | 0.1 |
| $K_2O$ | 0.5 | nd | nf | 0.0 | 0.0 | nd | nd | 0.2 | nd | 0.2 | 0.0 | nd | nd | nf | 0.0 | nf |
| $P_2O_5$ | 0.1 | 0.3 | 0.2 | 0.2 | nd | 0.1 | 0.1 | 0.2 | nd | nd | nd | nd | nd | nf | 0.2 | nf |
| Total | 99.1 | 100.0 | 99.9 | 100.1 | 98.6 | 99.4 | 99.9 | 100.0 | 100.5 | 100.0 | 98.5 | 98.8 | 98.3 | 100.4 | 99.8 | 100.1 |
| FeO Oivine | 2.1 | 1.4 | 0.6 | 2.5 | 2.5 | 1.6 | 3.4 | 2.0 | 1.8 | 2.7 | 2.4 | 3.0 | 2.3 | 1.4 | 3.6 | 1.9 |
| $Cr_2O_3$ olivine | 0.7 | 0.6 | 0.2 | nd | 0.6 | nd | 0.7 | 0.5 | 0.6 | 0.7 | 0.7 | 0.7 | 0.3 | 0.5 | 0.8 | 0.5 |
| Texture | Aggr POP | Aggr POP | Aggr MO | Aggr POP | Aggr PPO | Ch MO | Ch POP | Ch POP | Aggr POP | Ch POP | Aggr PPO | Aggr MO | IO | Aggr MO | Aggr POP | Ch POP |
| An (CT-°C) | 1305 | 1293 | 1319 | 1260 | 1260 | 1218 | 1293 | 1323 | 1305 | 1244 | 1242 | 1308 | 1178 | 1299 | 1275 | 1243 |
| An + Aug (CT-°C) | 1164 | 1167 | 1189 | 1155 | 1169 | 1180 | 1163 | 1165 | 1177 | 1152 | 1162 | 1163 | 1163 | 1183 | 1153 | 1146 |

Aggr = aggregate; Ch = chondrule; IO = isolated olivine; POP = porphyritic olivine-pyroxene; PPO = porphyritic pyroxene-olivine; MO = mosaic; nd = not determined; nf = not found; An (CT−°C) and An + Aug (CT−°C) = crystallization temperature of anorthite and anorthite + augite in °C.

[a] Glass inclusions with secondary-ion mass spectrometry analyses.

different stages in the history of the rock (Roedder, 1984). While the inclusions in, e.g., olivine, had to remain on an olivine subtraction line, the interstitial glasses in chondrules may have followed quite different lines of descent. All of our aggregates and chondrules have crystallized mesostasis, demonstrating a different history and evolution. Because of the crystalline nature of these mesostasis, no useful analyses for comparison with the glass inclusions could be obtained.

Nevertheless, we will compare the glass inclusions with glassy mesostasis from other chondritic meteorites: Kaba, Mezö Madaras (Kurat, 1967), Tieschitz (Kurat, 1971), Bishunpur, Semarkona, and Chainpur (Alexander, 1994). This comparison, however, has to be taken with care because glasses of glass inclusions and those of the interstitial mesostasis belong to different types of meteorites formed under different physicochemical conditions. In any case, this study mainly focuses on glasses of glass inclusions in olivine, as we believe that they are reliable recorders of the physicochemical conditions prevailing during olivine formation. Because all inclusions of this study in olivines of Renazzo, El Djouf, and Acfer 182 are primary glass inclusions as defined above, they carry information on the formation conditions of the host olivines which goes beyond the information that can possibly be extracted from the olivines themselves.

### 5.2. Mechanism of Formation of Glass Inclusions

Several processes have been considered for the formation of glass inclusions in olivines of chondritic meteorites. One model sees the glass inclusions in olivines as parental melt that was trapped during olivine crystallization during chondrule formation (McSween, 1977; Roedder, 1981). This model considers olivines as crystallization products of chondrule melts (Richardson and McSween, 1978; McSween, 1977) and also takes care of the isolated olivines and olivine aggregates by postulating that these may be fragments of former chondrules.

The second model sees the glass inclusions in olivines as remnants of a melt that was present when the olivines formed by condensation from a vapor. In this model, olivines are interpreted as high-temperature nebular condensates (Larimer and Anders, 1967; Grossman, 1972; Grossman and Olsen, 1974). In the extreme case and considering the chondrule formation model of Kurat (1988)—which envisions olivines formed by condensation to aggregate and form the protoliths for chondrules, which subsequently experienced part melting and shaping into droplets—all olivines could possibly carry a memory of their ultimate origin. In addition, there are the hybrid models which see only the inclusions in isolated olivines as condensation products but all others to be of igneous origin.

In this report we will try to accommodate the new data gathered on glass inclusions in olivine to one or several of the above-mentioned models.

#### *5.2.1. Are glass inclusions in olivines parental melts trapped during chondrule formation?*

Glass inclusions in olivines in terrestrial crustal rocks are considered to represent samples of the melt from which the host crystal formed. In a similar way, primary glass inclusions in olivines of chondrules are generally believed to be the product of fractional crystallization of chondrule melts. All glass inclusions studied here are hosted by olivines with low FeO contents (<3.6 wt.%, Table 1). Therefore the composition of these glasses can be compared to those found in olivines of type I chondrules by McSween (1977). Major element composition of glasses from Renazzo, Acfer 182, and El Djouf 001 shows that (except for the few Na-rich glasses) they are Si-Al-Ca-rich with a chondritic Ca/Al ratio and have low contents of FeO, MgO,

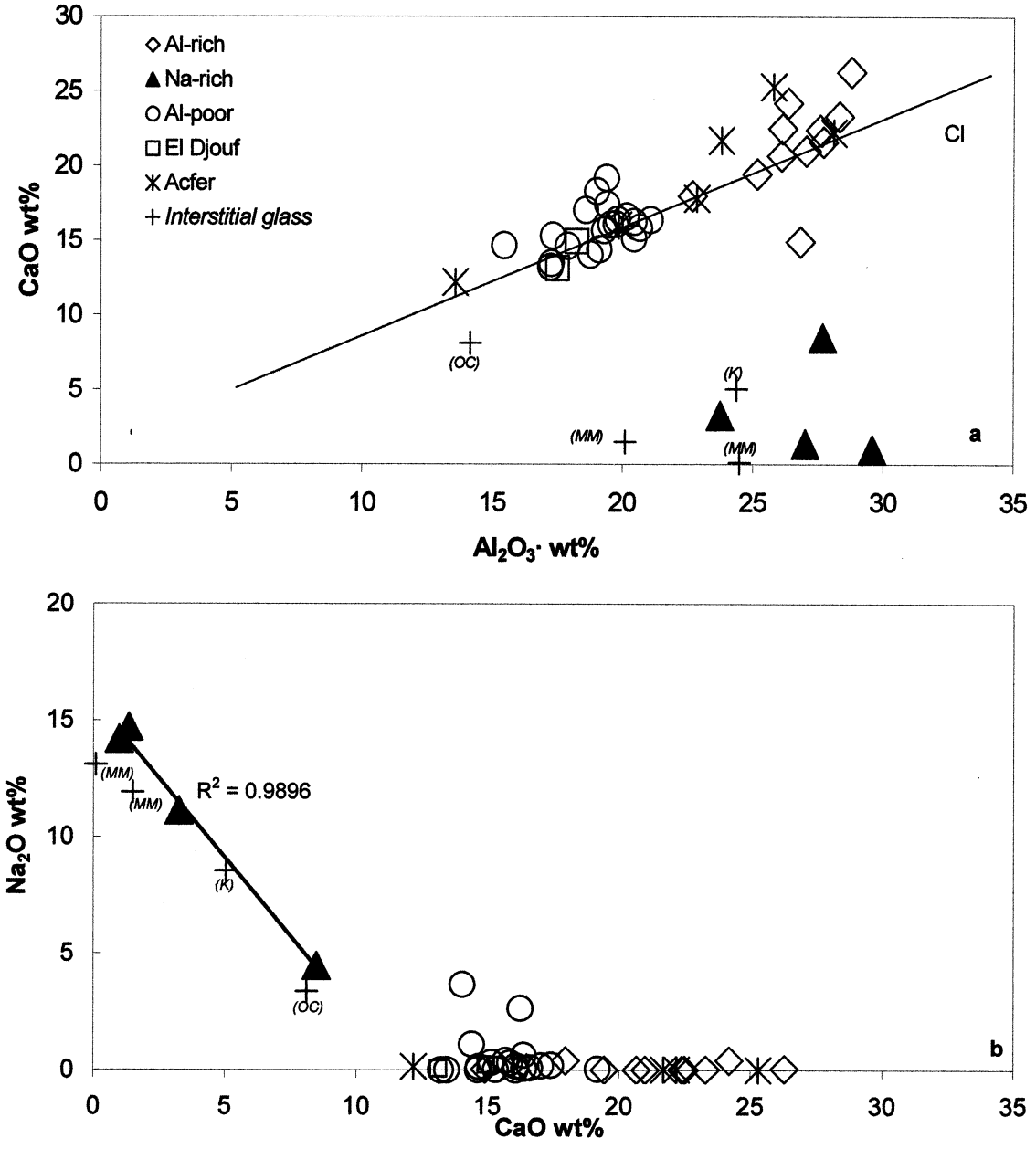


Fig. 2. Compositional variation diagrams of glasses of all types of glass-bearing inclusions in olivines from Renazzo, El Djouf 001, and Acfer 128. (a) CaO vs. $Al_2O_3$; the Al-rich and Al-poor glasses straddle the chondritic $CaO/Al_2O_3$ ratio line marked CI, the Na-rich glasses project off that line. Note clustering of Al-rich (around 27 wt.% $Al_2O_3$) and Al-poor (around 19 wt.% $Al_2O_3$) glass compositions. (b) $Na_2O$ vs. CaO; the Na-rich glasses have anticorrelated $Na_2O$ and CaO contents.

and $Na_2O$. They match the average composition of 11 glass inclusions from Murchison olivines (Fuchs et al., 1973). However, they differ from that of glasses of the glass inclusions in an isolate olivine and in a chondrule of the Kainsaz chondrite (McSween, 1977) as they have high contents of $Na_2O$ and a nonchondritic Ca/Al ratio. According to McSween (1977), glass compositions that plot into the plagioclase primary field (Fo-An-Qz system) lie approximately on an olivine subtraction line from the bulk composition of the trapped melt. Accordingly, "production of this glass as a residuum after crystallization of olivine requires that plagioclase does not nucleate when the liquid composition arrives at the olivine-plagioclase cotectic." Also, he indicates that for those glass inclusions with a composition near to pure anorthite (generally bytownite or anorthite) it may be difficult for a residual liquid composition trajectory to proceed to this extreme by fractional crystallization of olivine.

The Al-rich and Al-poor glasses form tight compositional clusters (Fig. 2) with a few transitional compositions. The normative mineral composition of the Al-rich glasses is silica-saturated (olivine-free) and is highly dominated by anorthite (An 74, Di 22 mol.%). The Al-poor glasses are silica-oversaturated (Q = 24 mol.%), contain 19 mol.% diopside and are also

Table 2. Trace element contents in glasses of glass inclusions and the host olivines. Secondary-ion mass spectroscopy (SIMS) data in ppm.

| | Al-rich R2 | *error ± ppm* | Al-rich R3 | *error ± ppm* | O12-3 | *error ± ppm* | Al-rich R5 | *error ± ppm* | O15 | *error ± ppm* | Al-rich R6 | *error ± ppm* | Al-rich R7 | *error ± ppm* | O16-7 | *error ± ppm* | Na-rich R15 | *error ± ppm* | Al-poor R27 | *error ± ppm* | O127 | *error ± ppm* | Al-poor R17 | *error ± ppm* |
|---|---|---|---|---|---|---|---|---|---|---|---|---|---|---|---|---|---|---|---|---|---|---|---|---|
| K | 111 | *2.5* | 363 | *3* | 5.6 | *0.1* | 36.2 | *2.8* | 21.8 | *0.9* | 103 | *5* | 46.6 | *3.26* | 37.9 | *1.2* | 13400 | *26* | 437 | *9* | 5.2 | *0.4* | 231.9 | *2.1* |
| Sc | 82.6 | *1.3* | 54.1 | *0.7* | 11.0 | *0.1* | | | | | | | | | | | | | | | | 57 | 0.6 | |
| Ti | 8255 | *85* | 6944 | *42* | 174 | *2* | 99.30 | *120* | 244 | *8* | 9130 | *120* | 3090 | *70* | 432 | *11* | 2200 | *27* | 5070 | *1* | 166 | *5* | 68.11 | *36.3* |
| V | 183 | *2.7* | 205 | *2* | 202.3 | *0.6* | 75 | *3* | 136 | *2* | 15.4 | *1.5* | 31.3 | *2* | 49.5 | *1.1* | 12.6 | *0.63* | 35 | *2* | 136 | *1.5* | 31.3 | *0.6* |
| Cr | 2149 | *14* | 2183 | *10* | 930 | *2* | 2640 | *22* | 5410 | *14* | 605 | *11* | 574 | *11* | 487 | *4* | 1820 | *9* | 2820 | *23* | 3750 | *9* | 2495 | *9.8* |
| Sr | 98 | *2* | 85.6 | *1.3* | 2.52 | *0.01* | 148 | *6* | 0.21 | *0.04* | 181 | *7* | 56.8 | *4* | 0.06 | *0.02* | 54 | *2* | 110 | *5.2* | 0.03 | *0.01* | 49.5 | *0.8* |
| Y | 27 | *1* | 21 | *0.6* | 0.24 | *0.02* | 27.3 | *2.1* | 0.227 | *0.04* | 32 | *2* | 12.5 | *1.5* | 0.53 | *0.05* | 25 | *1* | 19.3 | *1.7* | 0.15 | *0.02* | 35.9 | *0.7* |
| Zr | 77 | *3* | 66.5 | *1.9* | 0.07 | *0.02* | 74 | *5* | 0.234 | *0.06* | 82 | *6* | 41.5 | *4.3* | 0.17 | *0.05* | 9.5 | *3* | 53 | *5* | 0.11 | *0.03* | 45.9 | *1.3* |
| Nb | 6.1 | *0.8* | 5.9 | *0.5* | | | 5.5 | *1.5* | <0.07 | | <0.0 | | <1.5 | *0.4* | | | 4.2 | *0.7* | 7.6 | *1.7* | <0.05 | | 3.4 | *0.33* |
| Ba | 44.5 | *1.7* | 43.2 | *0.9* | 0.04 | *0.01* | 52.6 | *1.6* | | | 64 | *2* | 16.8 | *0.9* | 0.03 | *0.009* | 6.4 | *0.3* | 35.3 | *1.3* | 0.016 | *0.006* | 24.1 | *0.56* |
| La | 4.2 | *0.2* | 3.3 | *0.2* | | | 4.4 | *0.4* | 0.023 | *0.007* | 5.5 | *0.5* | 2.31 | *0.3* | <0.004 | | 6.0 | *0.2* | 2.9 | *0.3* | <0.002 | | 1.78 | *0.12* |
| Ce | 8.7 | *0.6* | 8.2 | *0.3* | 0.01 | *0.004* | 12.6 | *0.7* | 0.052 | *0.01* | 1.45 | *0.8* | 6.1 | *0.5* | <0.05 | | 16.1 | *0.4* | 9.7 | *0.6* | 0.01 | *0.004* | 5.1 | *0.2* |
| Pr | 1.39 | *0.22* | 1.15 | *0.11* | | | 1.5 | *0.3* | <0.01 | | 2.8 | *0.3* | 0.7 | *0.17* | <0.8 | | 2.74 | *0.15* | 1.3 | *0.2* | <0.26 | | 0.8 | *0.07* |
| Nd | 7.1 | *0.5* | 5.7 | *0.3* | | | 8.2 | *0.6* | 0.044 | *0.01* | 9.8 | *0.7* | 3.82 | *0.4* | <0.015 | | 11.1 | *0.3* | 7.0 | *0.5* | 0.01 | *0.004* | 3.9 | *0.18* |
| Sm | 2.7 | *0.5* | 1.85 | *0.19* | | | 1.3 | 0.5 | <0.02 | | 2.8 | *0.5* | 1.89 | *0.4* | 0.01 | *0.007* | 3.2 | *0.25* | 1.8 | *0.4* | <0.03 | | 1.4 | *0.15* |
| Eu | 0.84 | *0.18* | 0.56 | *0.08* | | | 1.1 | 0.2 | <0.01 | | 1.57 | *0.29* | 0.68 | 0.2 | <1 | | 0.27 | *0.06* | 1.2 | *0.2* | <0.009 | | 0.3 | *0.06* |
| Gd | 3.3 | *0.7* | 2.4 | *0.3* | 0.01 | *0.003* | 4.6 | 0.9 | <0.03 | | 5.3 | *1* | 2.46 | *0.6* | <0.02 | | 3.3 | *0.45* | 3.6 | *0.8* | <0.01 | | 2.52 | *0.29* |
| Tb | 0.54 | *0.15* | 0.44 | *0.07* | | | 0.8 | 0.2 | <0.4 | | 0.59 | *0.19* | <0.3 | *0.1* | <0.08 | | 0.74 | *0.1* | 0.67 | *0.17* | <0.007 | *0.48* | 0.06 | |
| Dy | 3.4 | *0.4* | 3.12 | *0.19* | 0.07 | *0.003* | 5.1 | *0.5* | 0.016 | *0.007* | 5.9 | *0.5* | 2.71 | *0.35* | 0.04 | *0.009* | 4.7 | *0.2* | 4.8 | *0.4* | <0.012 | *4.28* | 0.19 | |
| Ho | 0.98 | *0.19* | 0.62 | *0.08* | 0.01 | *0.003* | 0.82 | *0.18* | <0.01 | | 1.1 | *0.2* | 0.38 | *0.13* | 0.02 | *0.006* | 0.95 | *0.09* | 0.78 | *0.17* | 0.01 | *0.004* | 1.04 | *0.09* |
| Er | 2.3 | *0.4* | 1.92 | *0.17* | 0.02 | *0.005* | 3.7 | *0.4* | 0.016 | *0.007* | 3.3 | *0.4* | 1.16 | *0.25* | 0.09 | *0.015* | 3.2 | *0.2* | 2.2 | *0.3* | 0.02 | *0.007* | 3.53 | *0.19* |
| Tm | 0.24 | *0.10* | 0.36 | *0.06* | 0.01 | *0.003* | 0.34 | *0.12* | <0.01 | | 0.46 | *0.15* | 0.32 | *0.12* | 0.02 | *0.006* | 0.48 | *0.07* | 0.34 | *0.12* | <0.008 | | 0.48 | *0.06* |
| Yb | 2.3 | *0.3* | 1.83 | *0.16* | 0.06 | *0.009* | 2.9 | *0.5* | 0.075 | *0.016* | 2.8 | *0.5* | 0.62 | *0.24* | 0.14 | *0.02* | 3 | *0.2* | 2.8 | *0.4* | 0.08 | *0.01* | 3.2 | *0.18* |
| Lu | 0.43 | *0.16* | 0.22 | *0.07* | 0.01 | *0.003* | 0.42 | *0.18* | 0.023 | *0.009* | 0.78 | *0.23* | | | 0.03 | *0.01* | 0.61 | *0.11* | 0.35 | *0.16* | 0.02 | *0.006* | | |
| Hf | | | | | | | 5.1 | *2.2* | <0.3 | | <6 | | 3.43 | *1.4* | <0.5 | | 3.6 | *1.2* | 6.1 | *1.7* | | | | |

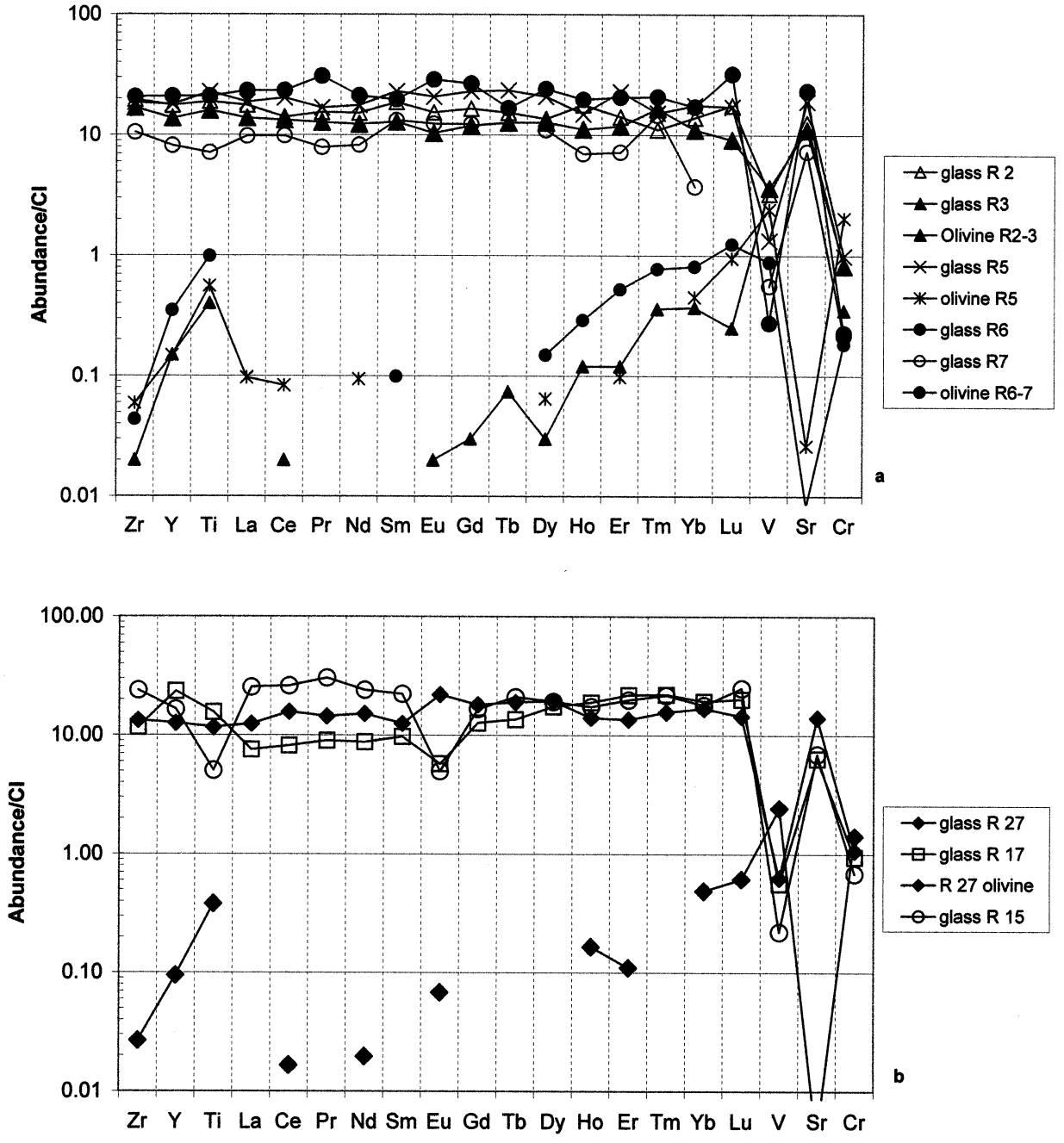


Fig. 3. (a) CI-normalized trace element abundances in Al-rich glasses (R2, R3, R5, R6, R7) of glass-bearing inclusions and their host olivines from the Renazzo chondrite. Normalization data from Anders and Grevesse (1989). (b) CI-normalized trace element abundances in Al-poor (R17, R27) and Na-rich (R15) glasses of glass-bearing inclusions and their host olivines from the Renazzo chondrite. Normalization data from Anders and Grevesse (1989).

dominated by plagioclase (54 mol.%, An91Ab8Or1). There seems to be a simple relationship between the Al-rich and Al-poor glasses: the chemical composition of the latter can be derived by adding ~30 mol.% silica to the Al-rich glass (the alkali contents are possibly of secondary nature). Because these two compositions cluster rather than show continuous mixing, they appear to have been buffered by a large reservoir that was silica-saturated in the case of Al-rich glasses and silica-oversaturated in the case of Al-poor glasses. Interestingly, in both cases olivine was precipitated and these olivines do not show any compositional differences.

Estimations of the glass crystallization sequences (Ariskin et al., 1997) for the Al-rich and Al-poor glasses predict in all cases plagioclase (mostly anorthite) to be the liquidus phase followed by augite (Fig. 4). The liquidus temperatures vary from 1647 to 1376°C for the Al-rich glasses and from 1323 to

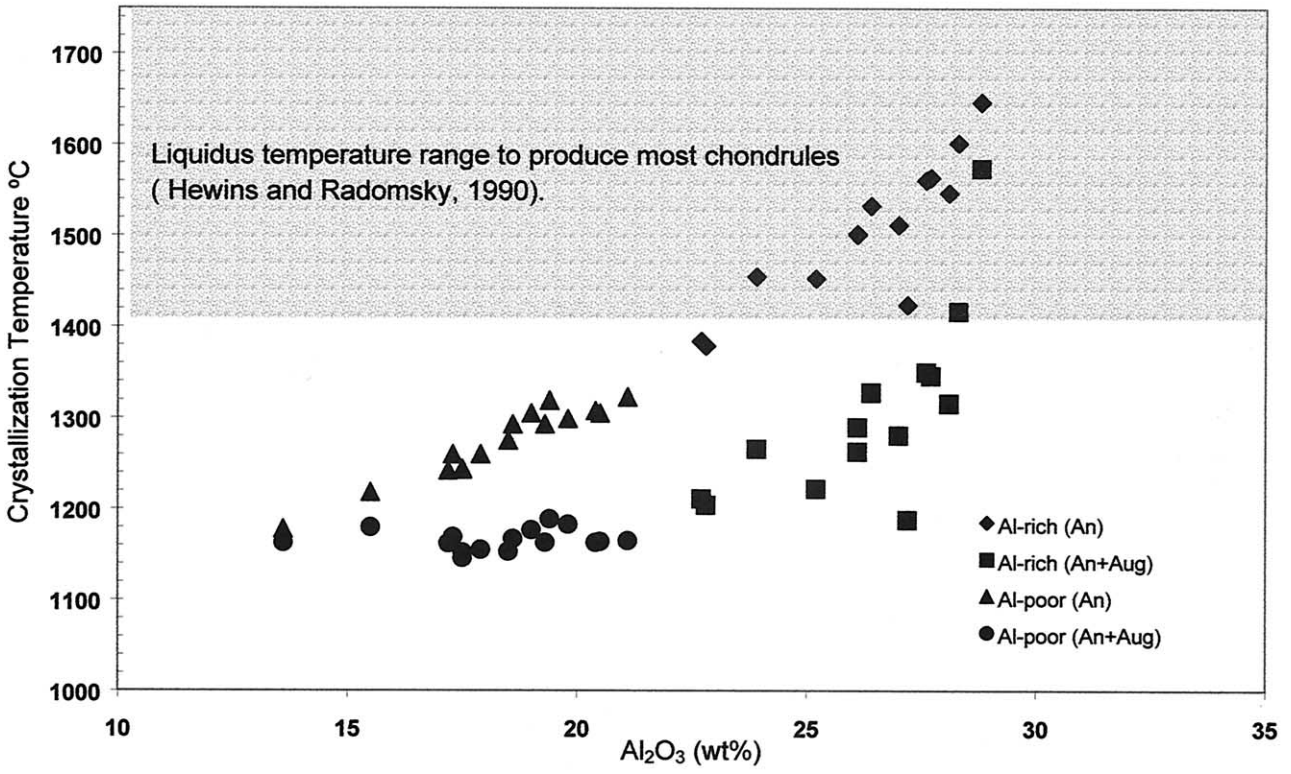


Fig. 4. Crystallization temperature (Ariskin et al., 1997) for anorthite and anorthite + augite from Al-rich and Al-poor glasses and the maximum initial temperatures to which chondrules could have been heated.

1178°C for the Al-poor glasses (Table 1). Augite joins the anorthite in the Al-rich glasses between 1574 and 1170 °C, that is, between 70 (R4, POP) and 270°C (R5, isolated olivine) below the liquidus. In the Al-poor glasses augite comes in between 1189 and 1070°C, 15 (Acfer2; isolated olivine) to 140°C (R16, POP) below the liquidus. None of the glasses of glass inclusions in olivine is multiphase saturated, a feature one would expect if they are residual melts. Instead, anorthite is the sole liquidus phase with the onset of augite crystallization thermally well separated in most cases by 100 to 200°C. Also, the liquidus temperatures are very high, especially those of the Al-rich glasses.

According to experimental studies (Hewins and Radomsky, 1990), few chondrules have liquidus temperatures above 1750°C and most chondrules may therefore have been heated to temperatures of 1400 to 1750°C. Most Al-rich glasses have liquidus temperatures that match those of olivine-rich chondrules (Fig. 4). However, the missing olivine saturation (all glasses) and the silica oversaturation (Al-poor glasses) also point toward an independent genesis of glass inclusions and olivines. The tight compositional clusters shown by the Al-rich and Al-poor glasses record different environments which appear to have been buffered by large reservoirs that did not allow a continuous chemical evolution. The Al-poor glasses must have been formed at lower temperature than the Al-rich ones.

#### *5.2.2. Calcium partitioning between olivine and glass*

The latest results in calcium partitioning between olivine and melt in a magmatic environment show that "systematic variations of the calcium content of olivine may be used as an in situ chemical potentiometer of the lime activity of the melt" (Libourel, 1999). These data can also be used to test whether equilibrium was achieved between olivine and melt. Figure 5 presents the Ca content of olivine in equilibrium with a melt. Our data for olivines and glass inclusions plot close to the equilibrium curve, indicating that olivines likely grew from melts with a composition similar to that of the glasses. However, as our data plot somewhat off the equilibrium curve for the CMAS (CaO, MgO, $Al_2O_3$, $SiO_2$) system (for details see Figure 6 from Libourel, 1999), they suggest (attempted) equilibrium at subliquidus temperatures, indicating either formation at or reequilibration under subliquidus conditions. The fact that olivines and their glass inclusions seem to be close to chemical equilibrium excludes the possibility that olivines crystallized from a melt of bulk chondritic composition because in this case olivines should be poor in Ca (and Al and Ti). Consequently, olivines with high Ca, Al, and Ti contents cannot have been derived from chondrules as these have on average chondritic lithophile elemental abundances.

### 5.3. Is the Chemical Variation of Glasses Related to the Alteration of Chondrules or to the Alteration of Olivine Before Chondrule Formation?

The title of this part of the discussion points towards the possibility that olivines could have formed before chondrule formation (that is, as a chondrule precursor) and be subsequently altered. Let us begin with a look at isolated olivines, the

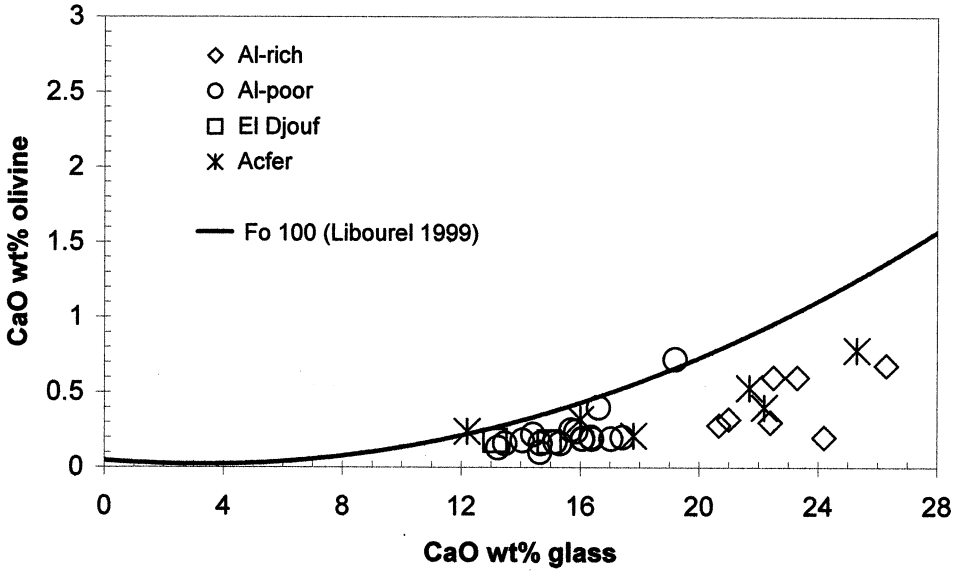


Fig. 5. CaO concentrations in glasses of glass-bearing inclusions and their host olivines. The liquidus equilibrium curve for the CMAS (CaO, MgO, $Al_2O_3$, $SiO_2$) system of Libourel (1999) is shown for comparison.

origin of which is a matter of debate between the igneous hypothesis, which considers them to be the product of crystallization from a melt (McSween, 1977; Zanda et al., 2000), or the nebular hypothesis which states that they formed by condensation in the solar nebula (Grossman and Olsen, 1974; Steele, 1988; Kurat et al., 1989).

According to the igneous hypothesis, the isolated refractory olivines could be derived from chondrules that were broken up. For a long time it was well established that chondrule olivines had different O isotope abundances than isolated olivines (Weinbruch et al., 2000) which tend to be rich in $^{16}O$. Only recently some examples of $^{16}O$-rich olivines have been found in chondrules (Jones et al., 2000; Leshin et al., 2000). The fact that the majority of chondrule olivines are isotopically different from isolated olivines still argues against an igneous origin of the latter. The presence of a few $^{16}O$-rich olivines in chondrules is perfectly compatible with the chondrule formation model of Kurat (1988).

The fact that isolated olivines contain Ca-Al-rich glass inclusions has been used by McSween (1977), Roedder (1981), and Zanda et al. (2000) as evidence for the derivation of isolated olivines from a Ca-Al-rich melt. But as discussed above, the chemical composition of glasses of glass inclusions appears difficult to reconcile with their formation by fractional crystallization of chondrule melts.

Many studies indicate that chondrules were formed from preexisting phases (Gooding and Keil, 1981; Grossman and Wasson, 1982; Kurat, 1984). According to thermodynamic calculations (Larimer and Anders, 1967; Grossman, 1972; Palme and Fegley, 1990), experiments performed at high temperature (Dohmen et al., 1998), and petrologic studies of different types of meteorites (Kurat, 1988), the precursor olivines are prone to have formed by condensation in the solar nebula. Pure forsterite seems to be always the first olivine to condense, even under very oxidizing conditions (Palme and Fegley, 1990). Also for the Mg-rich isolated olivines an origin by condensation from the solar nebular has been suggested (Steele, 1986; Palme et al., 1986; Kurat et al., 1989; Weinbruch et al., 2000). Thus, pure forsterite can be the first silicate phase formed by condensation. Then, one of the questions to be addressed is whether the secondary processes that can take place during and subsequently to chondrule and aggregate formation could, to some extent, also affect the primary glass composition.

The degree of alteration of the chondrules and aggregates that contain the host olivines of glass inclusions in the CR chondrites varies widely. In El Djouf and Acfer 182, mesostasis are free of any apparent alteration as are most of them in Renazzo. Glasses of glass inclusions in chondrule, aggregate, and isolated olivines belong to either the Al-rich or the Al-poor chemical glass group (Table 1). Thus, the chemical variation of glass inclusions seems to be independent of the occurrence of their host. Therefore, the possibility exists that the chemical variation of glasses is related to secondary processes that could have affected the host olivines.

We envisage that exchange reactions between the nebular vapor and the crystal took place before the formation of the chondrules or aggregates or they could have affected different olivine grains to different degrees. Thus, it could be interesting to inspect the variations of elements such as Na, Mn, or Cr that could effectively be involved during exchanges reactions.

Sodium has a low condensation temperature (50%, ~970 K at $10^{-4}$ bar, Palme et al., 1988) as compared to the refractory elements (e.g., Ca, Al) and Si that are the main components of glasses. The Na-rich glasses have Al contents comparable to those of the Al-rich glasses but their $CaO/Al_2O_3$ ratio deviates strongly from the chondritic ratio (Fig. 2a). Thus, it appears that Na has been incorporated into the glasses by secondary processes. A metasomatic exchange between the glass in the olivine and the vapor phase of Na for Ca is possible, similar to what has previously been observed in anorthite of Lancé basaltic objects (Kurat and Kracher, 1980).

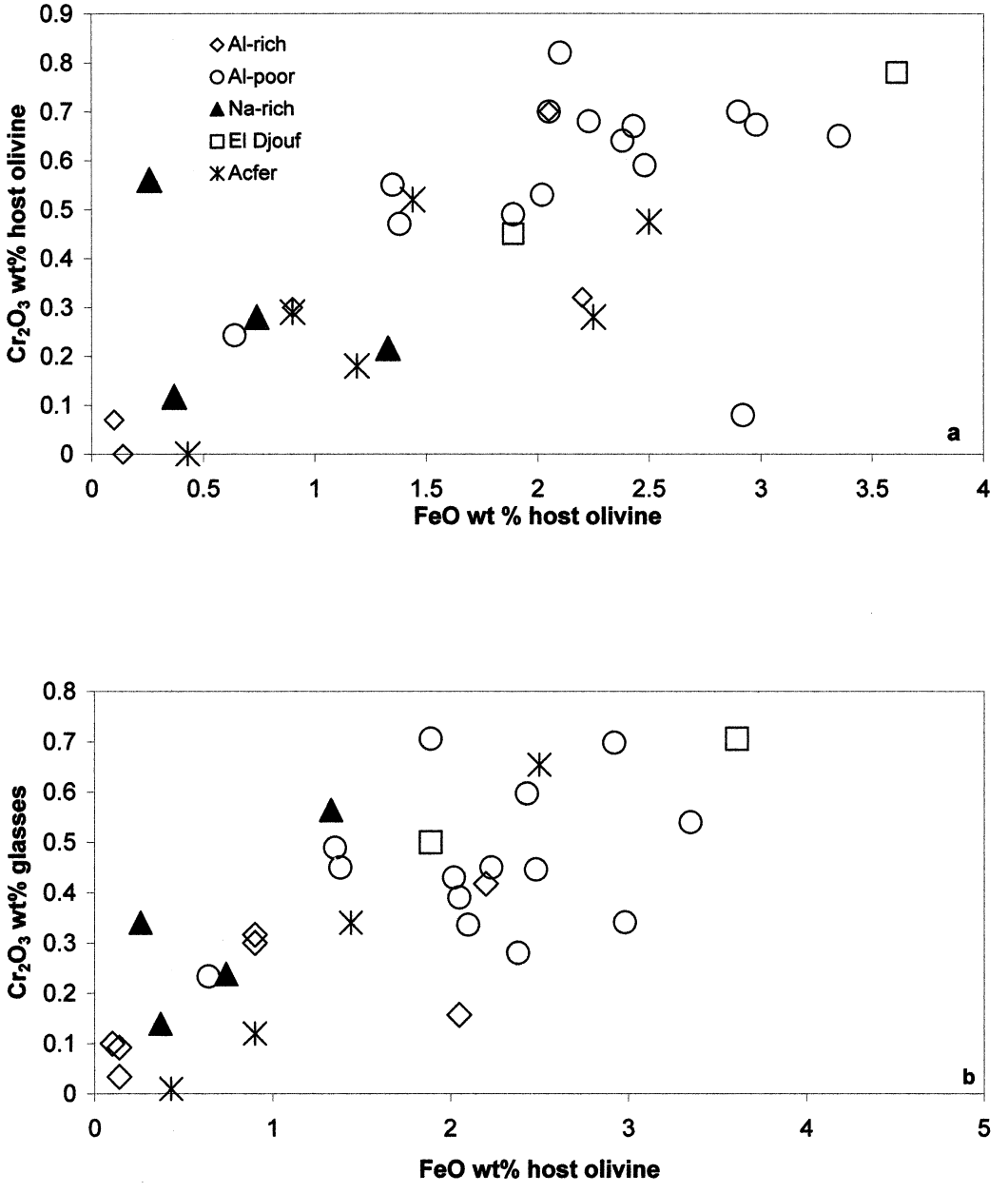


Fig. 6. Compositional variation diagrams of (a) $Cr_2O_3$ vs. FeO in glass-bearing inclusion host olivines and of (b) $Cr_2O_3$ in glasses of primary glass inclusions vs. FeO in host olivines from the Renazzo, El Djouf 001, and Acfer 128 CR chondrites.

Kong et al. (1999) concluded from the difference in the contents of Na and K in the matrix and chondrules of Renazzo and Al Rais (Weisberg et al., 1993; Osborn et al., 1974; Kong and Palme, 1999) that the volatile elements could have been evaporated from chondrules and recondensed onto the surface of any grain in the CR formation region. Thus, the enrichment of Na in glasses included in olivine could also have taken place before chondrule alteration. If Na was available and effectively deposited onto the surface of grains, then fractures in the olivine that can reach glass inclusions could be the passage through which Na could have been transported to the glasses. Indeed, glasses rich in Na are also generally associated to fractures (Fig. 1c).

Additional information can be obtained from glass inclusions hosted by isolated olivines. The isolated olivines that contain the glass inclusions R5, Acfer2, and Acfer3 have similar contents of FeO suggesting that they have seen similar redox conditions during their history. However, these three olivines are the hosts of glass inclusions with very different chemical composition (Al-rich and Al-poor, Table 1). This suggests that the Al-poor as well as the Al-rich glasses have both original compositions and that these chemical variations in glasses could have been established before aggregation.

If alterations took place, then elements such as Fe, Mn, and Cr must have been involved too. Metasomatic exchange reac-

tions between the ambient vapor and the olivine increase the contents of these elements in the olivines at the expense of Mg (Kurat, 1988; Dohmen et al., 1997). The roughly positive correlation of Fe and Cr contents in glasses and the olivine host (Fig. 6a,b) supports a metasomatic addition of Fe and Cr to the olivine and the glass. In summary, the primitive refractory composition of the primary glass inclusions in olivine could have been slightly modified due to solid-vapor exchange reactions that took place during the early stage of the chondrule precursor alteration.

### 5.4. Chemical Variations in Glass Inclusions: Evidence for Exchange Reactions with the Ambient Vapor

All Na-poor glasses of primary glass inclusions have a chondritic $CaO/Al_2O_3$ ratio (Fig. 2a) and unfractionated REE abundance (Fig. 3a, b) which suggest a primitive origin by condensation. The Na-rich glasses have similar contents of $Al_2O_3$ as those of the Al-rich group but have lower contents of CaO (Fig. 2a), indicating that Na-rich glasses could have been derived from the Al-rich group by loss of CaO and gain of Na. As has been suggested before (Kurat and Kracher, 1980; Kurat, 1988), Ca can be replaced by Na. The good anticorrelation of $Na_2O$ and CaO contents in glasses suggests that such an exchange took place (Fig. 2b). The correlation line of the Na-rich glasses points, however, towards the Al-poor group and not to the Al-rich group (as observed in Fig. 2a) as the possible parent for these glasses. Thus, the correlation line for Na-rich glasses has increased its slope possibly by an additional loss of Ca.

As mentioned previously, Cr appears to be another element that could have been incorporated into glasses via a secondary process. Chromium seems to have entered both the Al-rich and the Al-poor glasses (the enrichment of glasses in Cr almost doubles that of Fe, Fig. 7a). However, the possibly even more oxidizing conditions apparently prevailing during the Ca-Na exchange reactions as compared to those prevailing during Fe and Cr metasomatism, have favored addition of $Fe^{+2}$ over $Cr^{+3}$ to the Na-rich glasses (Fig. 7a).

Also, Ca and Cr seem to have been exchanged, as is suggested by the anticorrelation of their abundances in the glasses (Fig. 7b). This exchange reaction seems to have been more effective in the glasses of the Al-rich group as compared to all others. However, under apparently extreme conditions (maybe lower temperatures and increasing oxidation), the Na-rich glasses lost their Cr and gained Na. Sodium apparently replaces Cr and Ca (Fig. 7b,c), supporting the suspicion that Na-rich glasses could have suffered an additional Ca loss.

With respect to refractory elements, recent studies of chondrules and the chondrite matrix of Renazzo showed a strong Ti-Al fractionation between these two reservoirs (Klerner and Palme, 2000; Palme and Klerner, 2000). Chondrules and chondrite matrix have superchondritic and subchondritic Ti/Al ratios, respectively, whereas the bulk meteorite has, on a mm scale, a chondritic Al/Ti ratio (Palme and Klerner, 2000). The glass inclusions show also a Ti/Al fractionation. This ratio deviates from that of CI chondrites but in a symmetric way with the mean ratio of the different glasses remaining approximately chondritic (Fig. 8). This could indicate that a high-temperature solid Ti-rich phase was unevenly sampled by the glass during formation of the glass inclusion. The Na-rich glass of inclusion R15 (Fig. 3b and indicated by an arrow in Fig. 8) is the only one with a depletion in Ti relative to the other refractory elements. However, this glass is also depleted in Ba and Eu with respect to refractory elements, suggesting that the glass condensed at high temperature. The low Ti content, therefore, appears to be a primary feature. The high Na content consequently must be of secondary nature.

The fact that all types of glasses show similar variations of the Ti/Al ratio around the chondritic line indicates that they could have sampled either a Ti-rich condensate phase or the compositionally complementary Ti-depleted vapor. The range in the deviation of individual glasses from the chondritic Ti/Al line covers, in part, that observed in chondrules and the chondrite matrix of the Renazzo meteorite by Klerner and Palme (2000) (Fig. 9). This shows that primitive glasses were able to sample the Ti/Al variation occurring during the chondrule precursor formation. This information also supports the chondrule formation model of Palme and Klerner (2000) by which the Ti/Al fractionation requires the presence of a solid Ti-rich phase, possibly perovskite, among chondrule precursor components.

With respect to the interstitial glasses, their Na and Ca contents match the trend followed by the Na-rich inclusions (Fig. 2b), suggesting that they could have also been affected by Na-Ca exchange reactions. However, their low content of $Cr_2O_3$ compared to that of the Na-rich glass inclusions (Fig. 7c) and their highly variable contents of FeO (Fig. 7a), in addition to their subchondritic Ca/Al (Fig. 2a) and Ti/Al (Fig. 8) ratios, indicate that these glasses represent a different system to that of the primary glass inclusions.

### 5.5. Trace Element Abundances in Glasses Support Formation by Condensation

Host olivines of all glass inclusions are poor in LREE but have HREE contents which approach those of bulk chondrites (from 0.4 $\times$ CI to 1 $\times$ CI, Fig. 3a, b). Olivines also have high contents of Y and Ti (0.1 $\times$ CI to 1 $\times$ CI). Thus, trace element contents of the host olivines are fairly high but have fractionated abundance patterns according to elemental incompatibility.

Trace element abundances in glasses of glass inclusions of the Al-rich and of the Al-poor group are unfractionated and at $\sim$10 to 20 $\times$ CI abundances (Fig. 3a, b). If glass inclusions are remnants of a parent melt, we can expect some fractionation of the trace elements in the glass. However, the flat CI-normalized patterns, similar to those previously found by Kurat et al. (1997) for two glass inclusions (R2 and R3, Table 1), support that glass inclusions are very likely the product of a condensation process. The CI-normalized abundances of refractory trace elements in the Al-rich glass inclusions are unfractionated, with moderately volatile Cr and V depleted. The negative anomaly in V abundance, observed in all glass inclusions, could suggest that condensation took place under reducing conditions (Kurat et al., 1997).

Glass R7 has a pronounced positive anomaly in the abundance of Tm and a negative one in that of Yb. This could be a weak signal of a group II CAI REE abundance pattern. Such patterns can only be produced by condensation from a vapor that was depleted in the super-refractory REE. Either glass R7

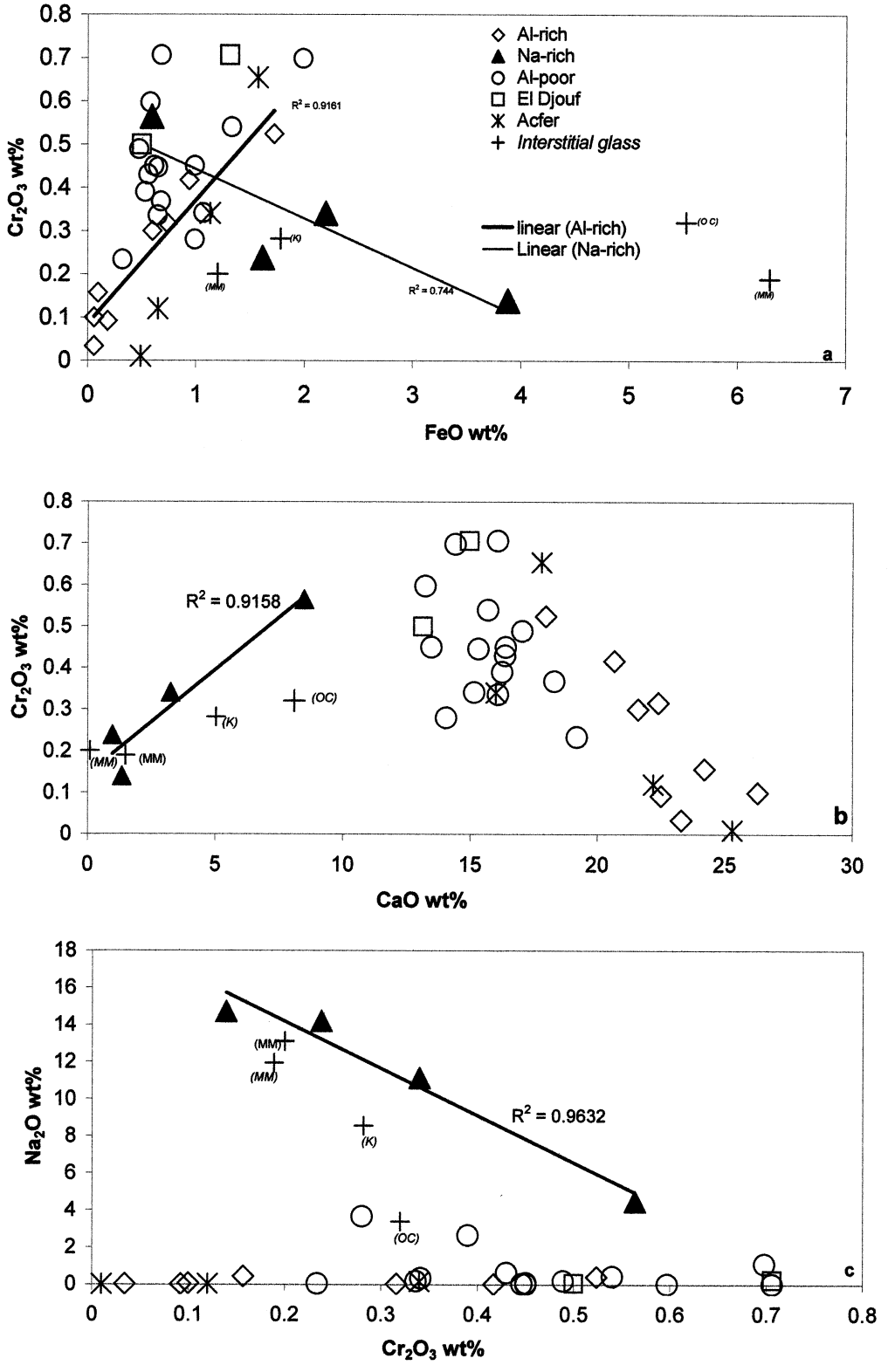


Fig. 7. Compositional variation diagrams of (a) $Cr_2O_3$ vs. FeO, (b) $Cr_2O_3$ vs. CaO, and (c) $Na_2O$ vs. $Cr_2O_3$ in glasses of glass-bearing inclusions of the Renazzo, El Djouf 001, and Acfer 128 CR chondrites. Black lines are correlation lines for chemical subgroups of glasses.

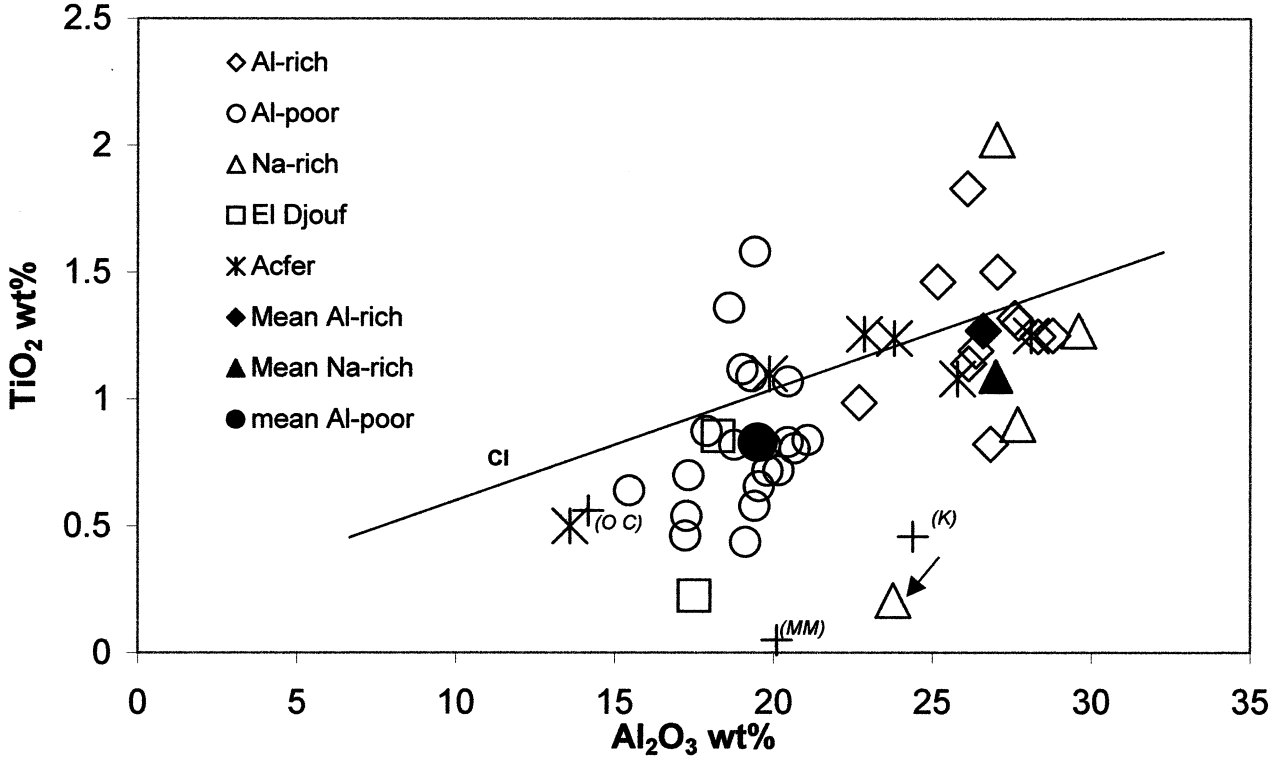


Fig. 8. Contents of $TiO_2$ vs. $Al_2O_3$ of glasses of glass-bearing inclusions from Renazzo, Acfer 128, and El Djouf 001. The solid line represents the chondritic $TiO_2/Al_2O_3$ ratio.

condensed from such a vapor or it collected such a condensate. Interestingly, glass inclusion R7 is hosted by an olivine that also hosts inclusion R6. The latter has not only much higher trace element contents than the former, it has unfractionated refractory trace element abundances (the abundance of Lu is within the same range when the analytical error is taken into account; Fig. 3a). Apparently, conditions did change considerably during growth of that particular olivine.

Olivine and inclusion glass trace element abundances approximately follow the olivine–liquid distribution coefficients (Green, 1994). However, olivine and inclusion glass seem not to be equilibrated as trace element abundances in the olivine require coexisting liquids with very high contents of Zr and Sm (~100 × CI) and Ti, Y, and Lu (~50 × CI). The contents of V and Cr in olivine and glass seem to be approximately in equilibrium. This is an interesting situation as the primary trace elements obviously are out of equilibrium but the secondarily introduced Cr is not.

The refractory trace element abundances of the Al-poor and Na-rich glasses are also at ~10 to 20 × CI abundances and have mostly unfractionated abundance patterns. Glass R15 (Na-rich) has the highest trace element content of all and flat, unfractionated normalized abundances of refractory lithophile elements, except for Ti and Eu which are less abundant (as is Ba). The missing Ti and Eu could indicate separation of carrier phases (perovskite and melilite, respectively) from the system before formation of the inclusion. The small difference in normalized abundances between the HREE (~20 × CI) and LREE (~30 × CI) could also be the result of separation of a super-refractory phase from the system before glass (and olivine) precipitation. The very low V content of glass R15 supports that view.

Glass R17 (Al-poor) is the only glass encountered that has fractionated REE abundances (Fig. 3b). The HREE are more abundant (~20 × CI) than the LREE (~8 to 10 × CI) and Eu is depleted relative to the other REE. In addition, the relative abundances of Ti, Y, and Zr are fractionated with Ti and Zr being depleted relative to Y. The relative abundances of HREE, Y, and Ti (and Eu) could indicate a super-refractory nature of the glass; the missing Zr, however, contradicts this view. Therefore the possible scenario could be: removal of perovskite (Ti and Zr), melilite (Eu), and an unknown phase with abundances of LREE > HREE from the system before glass (and olivine) formation.

The Al-poor glass R27 has approximately unfractionated abundances of the refractory lithophile elements and Sr. The coexisting olivine is very poor in trace elements. Their abundances follow approximately the olivine–liquid partition coefficients (Green, 1994) but seem not to be equilibrated as Ti, Y, and Zr indicate a coexisting liquid with ~10 to 20 × CI abundances but Ce and Lu one with 400 × CI and 100 × CI abundances, respectively. Vanadium seems to be overabundant in the olivine (partition coefficient ~2 to 3) whereas Cr appears to be in equilibrium (partition coefficient ~1) with that of the glass. As in the case of Al-rich glasses, the host olivine seems to be out of equilibrium with respect to the refractory elements (presumably of primary origin) but not with respect to the secondarily introduced elements like Cr.

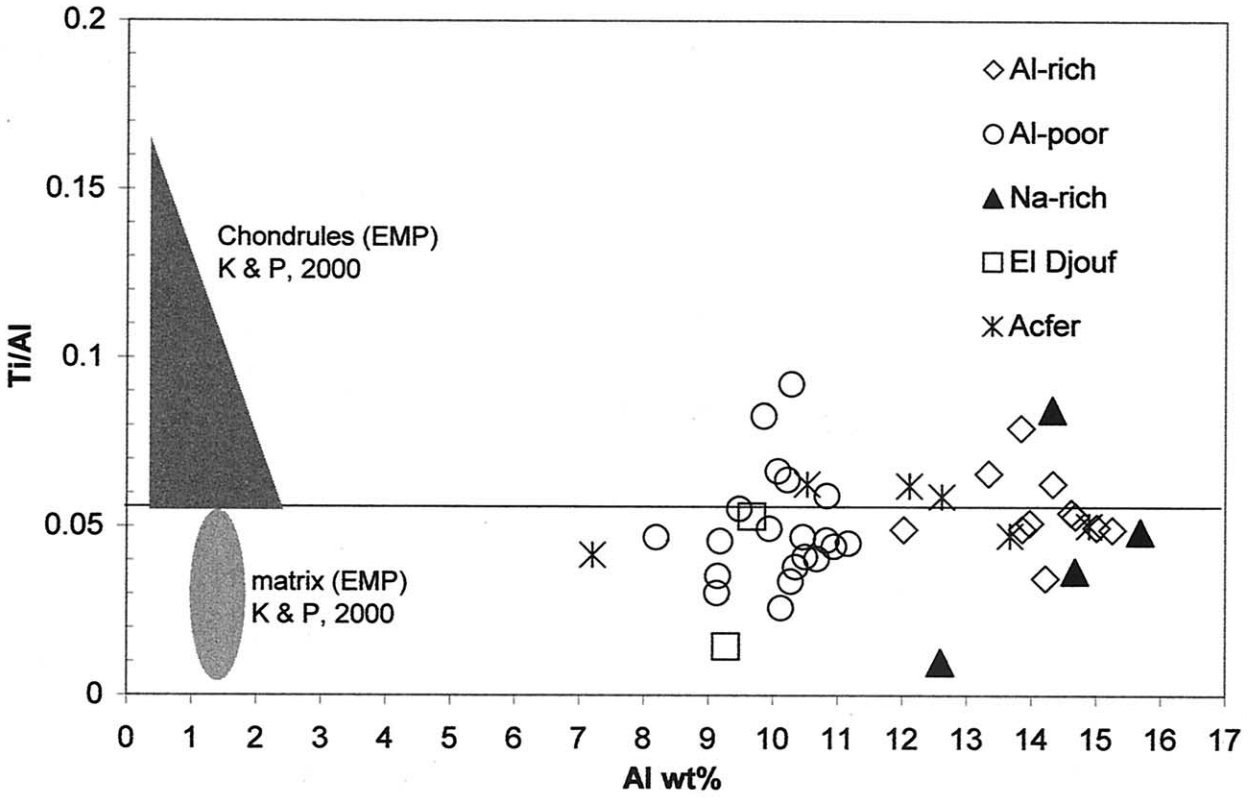


Fig. 9. Ti/Al ratio vs. Al concentration in glasses of primary glass-bearing inclusions from Renazzo, Acfer 128, and El Djouf 001. Note that deviations of individual glasses from the chondritic Ti/Al ratio line cover, in part, that observed for chondrules and the chondrite matrix of the Renazzo chondrite by Klerner and Palme (2000).

### 5.6. Phases That Could Have Acted as Nuclei for Glass Inclusion Formation

Any irregularity during growth of a crystal will favor the entrapment of foreign matter (Roedder, 1984). Any solid object at the growing surface of a crystal may also cause the formation of a glass inclusion by acting as a nucleation site for a liquid droplet. Spinel is frequently present as euhedral crystals in glass inclusions in olivines of different meteorites. The glass inclusion Acfer1 has a spinel crystal that occupies more than 30% of the inclusion cavity. Despite this, the glass has chondritic $CaO/Al_2O_3$ and $TiO_2/Al_2O_3$ ratios. If spinel formed as a daughter crystal from the melt, the Ca/Al and Ti/Al ratios of the glass would have been strongly fractionated. This is not the case and clearly shows that the spinel crystal did not grow from the melt which later became the glass but rather was trapped together with the glass. Thus, it is probable that the spinel grain acted as a nucleus for the medium that formed the glass inclusion. This was also recognized by McSween (1977), and he interpreted the fact that spinels are not daughter crystals but rather trapped crystals to favor the crystallization sequence subtraction of olivine with minor spinel and failure of nucleation of plagioclase for the formation of glass inclusions. However, spinel crystals can have acted as nuclei for the formation of glass inclusion by condensation, as spinel has a condensation temperature clearly higher (1503 K) than that of olivine (1443 K for $P_{tot} \sim 10^{-3}$ atm, Yoneda and Grossman, 1995).

Another phase that could have acted as a nucleus for glass inclusion formation could have been a Ti-rich phase. The Ti/Al ratio of glasses deviates in a symmetric way from the chondritic Ti/Al line. This suggests that during glass inclusion formation, Ti-rich solid phases could have been sampled in a stochastic way and could, naturally, also have served as condensation nuclei.

## 6. MODEL OF FORMATION OF GLASS INCLUSIONS

According to Yoneda and Grossman (1995), ". . .the presence of glass inclusions was difficult to reconcile with the proposed condensation model of their host forsterite grains because, up until that time, stable liquids were predicted by condensation models to be in equilibrium with forsterite in a solar gas only at total pressures greater then 100 atm (Wood, 1963), far higher than the maximum pressures allowed by hydrodynamic models of the solar nebula." However, they have shown that CMAS condensate liquids can be in equilibrium with forsterite at much lower total pressures and predicted that glass inclusions can be formed by condensation under certain nebular conditions. Here we propose a possible way to do so.

Crystals growing from the vapor need some support by a liquid to form a well-ordered crystalline phase—something like the vapor–liquid–solid (VLS) growth process (Givargizov, 1987; Kurat et al., 1997) or liquid-phase epitaxy. In this process, well-ordered and large crystals can grow from the vapor

with the help of a thin liquid layer bridging the vapor and the growing crystal. The liquid layer facilitates ordered growth of the crystal and acts as an accommodation surface because of its large accommodation coefficient (Givargizov, 1987). Consequently, those elements that will not easily enter the structure of the olivine, such as Ca, Al, and REE, will be concentrated in the vapor-crystal liquid interface. This liquid will have trace element contents which are diffusionally buffered by the vapor which at this stage is oversaturated in all refractory elements. These trace element contents will be independent of the crystal they are associated with. Part of this liquid will become glass inclusions as the interior of the growing crystal cools very fast by radiative heat transfer, thus quenching the liquid to glass.

One of the constraints of this model is that for developing the thin liquid interface, a total pressure higher than that of the canonical solar nebula is needed. As was suggested by Yoneda and Grossman (1995) and Ebel and Grossman (1999), glass inclusions could represent either liquids that were in equilibrium with forsterite at high pressures ($P_{tot}$ = 0.3 atm) or they could have been formed in regions governed by lower pressures ($P_{tot} = 10^{-3}$ atm) but with a dust/gas ratio ≈70 times the ratio of the conventional solar nebula. Such dust-enriched regions seem to provide the proper conditions for the formation of glass inclusions in early condensate phases like olivine. As these regions also have high partial pressures of O and all other elements, they also provide the right conditions for vapor–solid exchange reactions which led to enrichments of olivines and glasses in $Fe^{2+}$, $Mn^{+2}$, and $Cr^{+3}$. Also, the Ca-Na exchange reactions between the vapor and glasses could have been enhanced in oxygen-rich regions as oxidizing conditions are a prerequisite of mobilizing Ca as $Ca(OH)_2$ (Hashimoto, 1992).

Also, when a crystal is growing from the vapor, the growth rate is equal to the difference between the flux of atoms from the vapor to the crystal and the evaporation rate. As the flux of atoms is proportional to the vapor pressure (Pimpinelli and Villain, 1998), the dust-enriched regions with increased partial pressure of condensable species are favorable for the growth of sizeable crystals from the vapor.

Another question to be addressed is, if a crystal is grown from the vapor, how planes similar to those of pseudosecondary inclusions can be formed. In this case we have to invoke a type of growth similar to that of Stranski-Krastanov, where the layer-by-layer growth for the adsorbate (that is the olivine) is combined with the formation of droplets (Pimpinelli and Villain, 1998). In such a way, terraces form at the surface of the growing crystal which can give rise to the nucleation of melt droplets. The end product will have the appearance of an inclined and possibly warped plane containing several drops, a pseudosecondary plane of inclusions. However, considering that the great majority of glass-bearing inclusions in chondritic olivines is primary, this type of growth must have been rare.

## 7. CONCLUSIONS

Glasses of primary glass inclusions in olivines of the Renazzo, El Djouf, and Acfer 182 chondrites formed contemporaneously with the olivine. Three chemical groups can be distinguished: Al-rich, Al-poor, and Na-rich. The chemical variation of glass inclusions is independent of whether the host is an isolated olivine or is part of an aggregate or a chondrule. Apparently, all olivines had the same early (preaggregation?) history. They probably originated as condensates (as did the glasses), which is evidenced by their high contents of refractory lithophile minor and trace elements which are out of equilibrium with either the contents in the glass inclusions or the bulk chondrite. Moderately volatile elements, which likely were introduced into glasses and olivine by exchange reactions with the ambient vapor, have equilibrated distributions between glass and olivine host.

The Al-rich glasses are likely nebular condensates because they have unfractionated refractory lithophile element contents at ~10 to 20 × CI abundances. Glass R7 has a group II CAI–like trace element abundance pattern that indicates condensation from a fractionated vapor. The glasses richest (R6) and poorest (R7) in trace elements among the Al-rich glasses are present in one olivine, indicating changing conditions during growth of the olivine.

The Al-poor glasses have fractionated minor and trace element abundances (negative anomalies for Eu and Ti, fractionated Zr/Y ratio) which indicate removal of refractory phases from the vapor before glass (and olivine) precipitation (perovskite and melilite?).

The Na-rich glass R15 is also very rich in refractory lithophile elements and is depleted in Eu and Ti compared with the other refractory trace elements, indicating formation history similar to that of the Al-poor glasses. However, its Al content is similar to that of the Al-rich glasses, indicating a derivation from such a parent by exchange of Ca for Na with the ambient vapor.

Glass inclusions in olivine of CR-type chondrites possibly represent samples of the liquid which facilitated olivine growth from the vapor by the VLS process. The chemical compositions of inclusion glasses appear to be pristine except for the Na in Na-rich glass and the moderately volatile elements Cr, V, and Mn which possibly were acquired by solid–vapor exchange reactions (metasomatism). Glasses of glass inclusions therefore appear to be capable of keeping a record on processes that shaped olivines and possibly also chondrite constituents of CR-type and other chondrites.

*Acknowledgment*—We thank the late Marty Prinz (NHM, NY) for the thin section of El Djouf 001. We are grateful for the thorough reviews by R. Hewins and two anonymous referees and the constructive comments of the associate editor H. Palme. Financial support from the FWF (P-13975- GEO) and the Oskar und Friederike Ermann - Fonds, Austria, and CONICET and Fundación Antorchas (P-13887/81), Argentina, is gratefully acknowledged. M.E.V. wants to thank the Atomic Energy Commission of Argentina for providing access to the electron microprobe and A. Danon, R. Gonzalez, and V. Anzuli for assistance with the microprobe. We also thank Elmar Gröner for his assistance with the ion microprobe analyses at the Max-Planck-Institut für Chemie, Mainz, Germany.

*Associate editor:* H. Palme

## REFERENCES

Alexander C. M. O'D. (1994) Trace element distribution within ordinary chondrite chondrules: Implications for chondrule formation conditions and precursors. *Geochim. Cosmochim. Acta* **58,** 3451–3467.

Anders E. and Grevesse N. (1989) Abundances of the elements: Meteoritic and solar. *Geochim. Cosmochim. Acta* **53,** 197–214.

Ariskin A. A., Petaev M. I., Borisov, A. A., and Barmina G. S. (1997) A numerical model for the calculation of melting-crystallization relationships in metoritic igneous system. *Meteoritics Planet. Sci.* **32,** 123–134.

Bischoff A. (2001). Meteorite classification and the definition of new chondrite classes as a result of successful meteorite search in hot and cold deserts. *Planet. Space Sci.* **49,** 769–776.

Bischoff A., Palme H., Ash R. D., Clayton R. N., Schultz L., Herpers U., Stöffler D., Grady M. M., Pillinger C. T., Spettel B., Weber H., Grund T., Endreβ M., and Weber D. (1993) Paired Renazzo-type (CR) carbonaceous chondrites from the Sahara. *Geochim. Cosmochim. Acta* **57,** 1587–1603.

Dohmen R., Chakraborty S., Palme H., and Rammensee W. (1997) High-temperature formation of iron-oxide-rich olivine in the early solar system: Experimental simulation with thermodynamic and kinetic analysis of a solid-solid reaction mediated by a gas phase. *Meteoritics Planet. Sci.* **32,** Suppl. AA, A35–A36. (abstr.).

Dohmen R., Chakraborty S., Palme H., and Rammensee W. (1998) Experimental simulation of fayalitic rims on olivine: Kinetics constraints. *Meteoritics Planet. Sci.* **33,** Suppl. A, **A41,** (abstr.).

Ebel D. and Grossman L. (1999) Condensation in dust-enriched systems. *Geochim. Cosmochim. Acta* **64,** 339–366.

Fuchs L. H., Olsen E., and Jensen K. J. (1973) Mineralogy, mineral–chemistry and composition of the Murchison (C2) meteorite. *Smithson. Contrib. Earth Sci.* **10,** 38 pp.

Givargizov E. I. (1987) *Highly Anisotropic Crystals*. D. Reidel, Dordrecht, pp. 70–230.

Gooding J. L. and Keil K. (1981) Relative abundance of chondrule primary textural types in ordinary chondrites and their bearing on conditions of chondrule formation. *Meteoritics* **16,** 17–43.

Green T. H. (1994) Experimental studies of trace-element partitioning applicable to igneous petrogenesis: Sedona 16 years later. *Chem. Geol.* **117,** 1–36.

Grossman J. and Wasson J. T. (1982) Evidence of primitive nebular components in chondrules from the Chainpur chondrite. *Geochim. Cosmochim. Acta* **46,** 1081–1099.

Grossman L. (1972) Condensation in the primitive solar nebula. *Geochim. Cosmochim. Acta* **36,** 597–619.

Grossman L. and Olsen E. J. (1974) Origin of the high temperature fraction of C2 chondrites. *Geochim. Cosmochim. Acta* **40,** 149–155.

Hashimoto A. (1992) The effect of $H_2O$ gas on volatiles of planet-forming major elements: I. Experimental determination of thermodynamic properties of Ca-, Al-, and Si-hydroxide gas molecules and its application to the solar nebula. *Geochim. Cosmochim. Acta* **51,** 1685–1704.

Hewins R and Radomsky P. (1990) Temperature conditions for chondrule formation. *Meteoritics* **25,** 309–318.

Jones R. H., Saxton J. M., Lyon I. C., and Turner G. (2000). Oxygen isotopes in chondrule olivine and isolated olivine grains from the $CO_3$ chondrite, Allan Hill A77307. *Meteoritics Planet. Sci.* **35,** 849–858.

Kallemeyn G. W., Rubin A. E., and Wasson J. T. (1994) The compositional classification of chondrites: VI. The CR carbonaceous chondrite group. *Geochim. Cosmochim. Acta* **13,** 2873–2888.

Klerner S. and Palme H. (2000) Large Ti/Al fractionation between chondrules and matrix in Renazzo and other carbonaceous chondrites. *Meteoritics Planet. Sci.* **35,** Suppl. A89. (abstr.).

Kong P. and Palme H. (1999) Compositional and genetic relationship between chondrules rims, metal and matrix in the Renazzo chondrite. *Geochim. Cosmochim. Acta* **63,** 3673–3682.

Kong P., Ebihara M., and Palme H. (1999) Distribution of siderophile elements in CR chondrites: Evidence for evaporation and recondensation during chondrule formation. *Geochim. Cosmochim. Acta* **63,** 2637–2652.

Kurat G. (1967) Einige Chondren aus dem Meteoriten von Mezö-Madaras. *Geochim. Cosmochim. Acta* **31,** 1843–1857.

Kurat G. (1971) Die chemische Zusammensetzung von Gläsern und Chondrenmatrizes im Chondriten von Tieschitz. *Chemie Erde* **30,** 235–249.

Kurat G. (1984) Geochemistry of chondrules: Fractionation processes in the early solar system. *Proc. 27th Internat. Geol. Congr.* **11,** 155–197.

Kurat G. (1988) Primitive meteorites: An attempt towards unification. *Phil. Trans. R. Soc. Lond.* **A 325,** 459–482.

Kurat G. and Kracher A. (1980) Basalts in the Lancé carbonaceous chondrite. *Z. Naturforsch.* **35a,** 180–190.

Kurat G., Palme H, Brandstätter F., and Huth J. (1989) Allende xenolith AF: Undisturbed record of condensation and aggregation of matter in the solar nebula. *Z. Naturforsch.* **44a,** 988–1004.

Kurat G., Varela M. E., Hoppe P., and Clocchiatti R. (1997) Glass inclusions in Renazzo olivine: Condensates from the solar nebula? *Meteoritics Planet. Sci.* **32,** Suppl., A76. (abstr.).

Larimer J. W. and Anders E. (1967) Chemical fractionation in meteorites–II. Abundance patterns and their interpretation. *Geochim. Cosmochim. Acta* **31,** 1239–1270.

Leshin L. McKeegan K. D., Engrand C., Zanda B., Bourot-Denise M., and Hewins R. (2000). Oxygen-isotopes studies of isolated and chondrule olivine from Renazzo and Allende. *Meteoritics Planet. Sci.* **33,** No. 4 Suppl., A93–A94 (abstr.).

Libourel G. (1999) Systematics of calcium partitioning between olivine and silicate melt: Implications for melt structure and calcium content of magmatic olivines. *Contrib. Mineral. Petrol.* **136,** 63–80.

McSween H. (1977) On the nature and origin of isolated olivine grains in carbonaceous chondrites. *Geochim. Cosmochim. Acta* **41,** 411–418.

Métrich N. and Clocchiatti R. (1989) Melt inclusions investigation of the volatile behaviour in historic basaltic magmas of Etna. *Bull. Volcanol.* **51,** 185–198.

Osborn T. W., Warren R. G., Smith R. H. Wakita H., Zellmer D. L., and Schmitt R. A. (1974) Experimental composition of individual chondrites, including Allende. *Geochim. Cosmochim. Acta* **38,** 1359–1378.

Palme H. and Fegley B. Jr. (1990). High-temperature condensation of iron-rich olivine in the solar nebula. *Earth Planet. Sci. Lett.* **101,** 180–195.

Palme H. and Klerner S. (2000). Formation of chondrules and matrix in carbonaceous chondrites. *Meteoritics Planet. Sci.* **35,** Suppl. A124. (abstr.).

Palme H. Larimer J. W., and Lipschutz M. E. (1988) Moderately volatile elements. In *Meteorites and the Early Solar System* (eds. J. F. Kerridge and M. S. Matthews), pp. 436–461. Univ. Arizona Press.

Palme H., Spettel B., and Steele I. M. (1986) Trace elements in forsterite-rich inclusions in Allende. *Lunar Planet. Sci.* **17,** 640–641.

Pimpinelli A. and Villain J. (1998) *Physics of Crystals Growth.* Cambridge University Press, pp. 70–87.

Richardson S. M. and McSween H. Y. (1978) Textural evidence bearing on the origin of isolated olivine crystals in C2 carbonaceous chondrites. *Earth Planet Sci. Lett.* **37,** 485–491.

Roedder E. (1981) Significance of Ca-Al-rich silicate melt inclusions in olivine crystals from the Murchison Type II carbonaceous chondrite. *Bull. Mineral.* **104,** 339–353.

Roedder, E. (1984) Fluid inclusions. *Mineral. Soc. Am., Rev. Mineral.* **12,** 1–644.

Schiano P. and Bourdon B. (1999) On the preservation of mantle information in ultramafic nodules: Glass inclusions within minerals versus interstitial glasses. *Earth Planet. Sci. Lett.* **169,** 173–188.

Steele I. M. (1986) Composition and texture of relic forsterite in carbonaceous chondrites. *Geochim. Cosmochim. Acta* **50,** 1379–1395.

Steele, I. M. (1988) Primitive material surviving in chondrites: Mineral grains. In *Meteorites and the Early Solar System* (eds. J. F. Kerridge and M. S. Matthews), pp. 808–818. Univ. Arizona Press.

Varela M. E. and Kurat G. (2000). Glass inclusions in olivines of the Renazzo (CR) chondrite. *Meteoritics Planet. Sci.* **35,** Suppl. A162–A163. (abstr.).

Weinbruch S., Palme H., and Spettel B. (2000). Refractory forsterite in primitive meteorites: Condensates from the solar nebular? *Meteoritics Planet. Sci.* **35,** 161–171.

Weisberg M. K., Prinz M., Clayton R. N., and Mayeda T. K. (1993) The CR (Renazzo-type) carbonaceous chondrite group and its implications. *Geochim. Cosmochim. Acta* **57,** 1567–1586.

Wood J. A. (1962) Metamorphism in chondrites. *Geochim. Cosmochim. Acta* **26,** 739–749.

Wood J. A. (1963) On the origin of chondrules and chondrites. *Icarus* **2,** 152–180.

Yoneda S. and Grossman L. (1995) Condensation of Ca-MgO-$Al_2O_3$-$SiO_2$ liquids from cosmic gases. *Geochim. Cosmochim. Acta* **59,** 3413–3444.

Zanda B., Libourel G., and Blanc P. (2000). Blue luminescing olivine-fassaite-spinel chondrules in the Allende meteorite. *Meteoritics Planet. Sci.* **35,** No. 5. Suppl. A176–A177 (abstr.).

Zinner E. and Crozaz G. (1986) A method for the quantitative measurement of rare earth elements in the ion microprobe. *Int. J. Mass Spectrom. Ion Proc.* **69,** 17–38.